𝔄𝔯𝔤𝔬𝔫𝔫𝔢 𝔑𝔞𝔱𝔦𝔬𝔫𝔞𝔩 𝔏𝔞𝔟𝔬𝔯𝔞𝔱𝔬𝔯𝔶

PENETRATION AND CASCADE PHENOMENA

by

G. Zgrablich

ARGONNE NATIONAL LABORATORY
9700 South Cass Avenue
Argonne, Illinois 60439

PENETRATION AND CASCADE PHENOMENA

by

G. Zgrablich

Applied Mathematics Division

August 1970

TABLE OF CONTENTS

TABLE OF CONTENTS

LIST OF FIGURES

6

LIST OF TABLES

PENETRATION AND CASCADE PHENOMENA

by

G. Zgrablich*

ABSTRACT

This work treats two penetration-phenomena problems at low energies and two at very high energies:

1. The stopping probability in a material of a given thickness. The corresponding integro-differential equation is shown to have a regular solution accounting for a finite number of collisions, and a singular solution representing the contribution from an infinite number of collisions. The general solution is unique if and only if the singular solution is identically zero.

2. The ionization cascade produced by a charged particle. The distribution of ion-pairs produced is computed and can be approximated by the Landau universal distribution for energy loss by ionization. The mean number of ion pairs conditional on a given energy loss by the primary is shown to be linear and independent of primary energy, varying little with the nature of the absorber. The computed energy loss per ion-pair produced is in good agreement with experiments.

3. Multiple particle production models at cosmic-ray energies and their predictions for quantities such as inelasticity and multiplicity distributions. Special attention is paid to the two-temperature model.

4. The three-dimensional nucleon-pion cascade, solved by a semianalytical method, practical for numerical computation. The lateral structure function for the nuclear active component of extensive air showers is computed for several values of the incident energy and is compared to Monte Carlo calculations and to experimental results.

I. REVIEW OF PENETRATION PHENOMENA

A. Introduction

The observation of the phenomena that occur when a particle pene-
trates a material has been one of the main sources for fundamental dis-
coveries in modern physics and for the understanding of the structure of
matter and of particles themselves.

In general, since the effect of the material on the penetrating
particles is statistical in nature, one is interested in the probability dis-
tributions of their number and states, as a function of time or of the dis-
tance traveled, and quantities related to experimental observations that
depend on these distributions.

The large variety of collision events that should be taken into
account in a complete theory of the penetration of particles into matter
would make it impossible to obtain practical results. However, to a good
approximation, the effects of some types of collisions can be separated
from the effects of other types of collisions. Therefore we can consider
separately a number of penetration phenomena in each of which only a few
types of interactions are relevant to the quantities to be calculated. This
will become clear in Section B below when we discuss some of the main
types of collisions that can occur when energetic particles penetrate a
medium.

The discussion of these problems will be much simplified by the
following assumptions:

1. The total number of penetrating particles is much less than the
number of collision centers in the medium.

2. The effects of the particles on the medium are negligible; we
only consider the effects of the medium on the particles.

3. The collision events are independent of each other.

4. Collective effects are neglected (each collision event is con-
sidered as an isolated event).

5. The collision events are instantaneous.

As a result of the assumptions, we can split the mathematical prob-
lem into two steps: First, obtain the elementary probability distributions
for the collision events (differential cross sections), and then find the
probability distributions of the number of states of the particles. The
first part involves the physical analysis of the interaction process, the
second belongs to the classical statistical theory (assumptions 3 and 4
suggest the use of the theory of Markov processes).

B. Review of Collision Events

Two kinds of interactions, electromagnetic and strong, are of importance to penetration phenomena.

Electromagnetic interactions are, in general, well understood, and we will briefly summarize their main characteristics.

Strong interactions present challenging problems, especially at very high energies. Among them, the problem of multiple-particle production is of special interest for the penetration of particles into matter (in this case in the cosmic-ray showers phenomena) and will be discussed more extensively.

1. Electromagnetic Interactions

Different situations can be distinguished according to the impact parameter b of the collision (see Ref. 1 or 2):

a. $b \gg$ atomic distances

Here the spin of the colliding particle is not taken into account, and we consider the scattering with the atom as a whole.

b. $b \approx$ atomic distances

Here the main contribution comes from the inelastic scattering with atomic electrons. The main phenomenon that occurs is ionization. The results will be different, according to the mass and spin of the incident particle. If the energy loss is large, the electrons of the atom can be considered as free; otherwise, the binding energy should be taken into account. Compton and photoelectric effects occur if the incident particle is a photon.

c. $b \ll$ atomic distances

Here the nucleus plays the most important role as a scattering center.

The change in direction of motion of the incident particle becomes important because of the Coulomb interaction with the nucleus. Furthermore, two very important phenomena occur: bremsstrahlung (radiation process) and pair-creation (creation of a pair (e^+, e^-) by a photon).

All these types of collisions contribute with very different weights to the several phenomena one wants to describe.

Ionization phenomena, which are important at low energies ($<$ few MeV), are covered by collisions of types a and b. Here we are interested in obtaining the probability distributions of energy losses, ion pairs, and range. At low energy, collisions of type c do not intervene except for multiple scattering.

At higher energies (say $>10^8$ eV), we become more interested in cascade phenomena (electron-photon cascades) which are covered by collisions of type c. Here collisions of types a and b are unimportant; even the Compton effect is negligible in this case.

A quantitative and extensive coverage of electromagnetic interactions, as applied to penetration phenomena, appears in Refs. 1-3.

2. Multiple Particle Production at Very High Energy

Multiple production of particles in strong interactions begins at a few GeV. The particles that are capable of strong interactions are called <u>hadrons</u> (protons, neutrons, π mesons, K mesons, Λ particles, etc.).

Here we have only an empirical picture of the phenomenon and will summarize the main characteristics.

a. <u>Momentum Distribution of Secondaries</u>. To a good approximation, the longitudinal and transversal momenta in the center-of-mass system (CMS) can be considered as independent radom variables. Then the CMS momentum distribution can be expressed as a product $f(p_\ell^*)g(p_t^*)$. The CMS longitudinal momentum distribution $f(p_\ell^*) \, dp_\ell^*$ seems to follow an exponential law, say $(1/a) \exp(-ap_\ell^*)$; the CMS transversal momentum distribution $g(p_t^*)$ is better represented by

$$\text{const } p_t^{*3/2} e^{-bp_t^*},$$

where a and b are parameters of the interaction.

A striking feature is that the mean transversal momentum $\langle p_t^* \rangle$ is generally observed to be independent of the initial energy of the incident particle ($\langle p_t^* \rangle \approx 0.4$ GeV).

b. <u>Inelasticity</u>. Inelasticity is a random variable defined as $K^* = 1 - E/E_0$, where E is the energy carried away by the incident particle and E_0 is its initial energy. The inelasticity has a mean value which depends on the mass of the incident particle ($\langle K^* \rangle \approx 0.5$ for nucleons, ≈ 0.9 for pions) and has wide fluctuations.

c. <u>Multiplicity</u>. Multiplicity is a random variable which represents the number of secondary particles created in an interaction. Its mean value depends on the energy of the primary through either one of the laws

$$\langle n \rangle = \text{const } E_0^{1/4}, \quad \langle n \rangle = \text{const log } E_0.$$

(Experiments cannot distinguish between them.) As in the case of inelasticity, the multiplicity has wide fluctuations. Its distribution can be approximately expressed as $n^c e^{-dn}$, where c and d are parameters depending on the type of secondaries considered and on the primary energy.

In describing penetration phenomena in which strong interactions at very high energy occur (nucleon-pion cascade), collisions 1 and 2 of the electromagnetic interaction type are completely irrelevant and collisions 3 are rather complementary (nucleon-pion + electron-photon cascades). General review articles on these interactions, as related to cosmic ray showers, appear in Refs. 4 and 5.

In what follows we shall divide the discussion of penetration phenomena into two parts: low-energy and high-energy phenomena.

In Part One, two typical problems will be discussed: stopping probabilities and ionization cascades.

In Part Two, we shall analyze the multiple production of particles with special interest in the two-temperature model of high-energy interactions and then treat the three-dimensional nucleon-pion cascade problem.

In each chapter, one section will be dedicated to summarizing the results obtained, and this will be used instead of a general summary.

PART ONE

LOW-ENERGY PHENOMENA

II. STOPPING PROBABILITIES

A. Introduction

When a particle having energy E_0 enters a medium, it loses energy in the collisions with the atoms of the material and eventually stops. The thickness of material traversed by the particle until it stops is called the projected range R_p of the particle in the material. We shall use the term range generically to denote, in addition to the projected range:

     1.   The effective range R_e, which is the total path length traversed by the scattered particle.

     2.   The lateral range $R_\perp$, which is the distance from the end of the path of the particle to the axis perpendicular to the surface of the material through the point of penetration.

The relation between the various ranges is shown in Fig. 1.

For the same particle with the same E_0 in the same material, the range can take different values; that is, it shows fluctuations, and we are interested in its probability distribution (stopping probability).

Because of their importance in particle detection, radiation damage in solids, etc., range-energy relations have been extensively studied by several authors[6-9] from a phenomenological point of view.

Fig. 1. Representation of Stopping Ranges

Our aim is to present a systematic and rigorous treatment of stopping probabilities, based on the general theory of first-passage processes developed by Moyal.[10]

We will show that the stopping probability η satisfies an integral equation which reduces to the well-known backward integro-differential equation in the case of finite collision rate. We will briefly discuss the existence and uniqueness of solutions and solve the equation in some simple cases. It will turn out that η is a sum of two terms, η_R and θ_∞, where η_R is the regular solution of the integral equation and involves a finite number of collisions, and θ_∞ represents the contribution from an infinite number of collisions. The solution will be unique if $\theta_\infty \equiv 0$.

B. Integral Equation for the Stopping Probability

The idea of obtaining a general formulation for the stopping probability can be outlined as follows. We define the probability that a particle in a given state* makes its first passage through a general surface in the three-dimensional space. Then the total first-passage probability will be the probability that the particle makes its first passage through that surface in any state, and one minus this quantity will be the probability that the particle is stopped before making its first passage through the given surface.

Let X be the set of all possible positions x (the three-dimensional Cartesian space) and V (state space) the set of all intrinsic physical observables ν (i.e., momentum, energy, spin, etc.) of a given particle, and call the ordered pair $\omega = (\nu, x)$ its phase. The space $\Omega = V \times X$ will be the particle phase-space and $B(\Omega)$ a Borel field of measurable subsets Λ of Ω.

If $X(\tau)$ is a closed measurable subset of X bounded by a measurable surface τ, we can define a partially ordered set Γ of all surfaces τ by stating that $\tau_1 \geq \tau_2$ if $X(\tau_1) \supseteq X(\tau_2)$. We call $x(\tau)$ a point on τ, and $\omega(\tau) = (\nu, x(\tau))$ is the phase of a particle on τ. Then $\Omega(\tau) = V \times X(\tau)$, $\Sigma(\tau) = V \times \tau$, and $\Gamma(\tau)$ is a measurable subset of $\Sigma(\tau)$.

We can now define a first-passage process, according to Moyal,[10] as a family of first-passage functions P, which are conditional probability distributions on $B[\Sigma(\tau)] \times \Omega(\tau)$ satisfying the conditions

I.   For each fixed phase $\omega(\tau_0) \in \Omega(\tau)$, $P[\cdot \,|\omega(\tau_0)]$ is an incomplete probability distribution on $B[\Sigma(\tau)]$.

II. For each fixed set $\Gamma(\tau) \in B[\Sigma(\tau)]$, $P[\Gamma(\tau)|\cdot]$ is a measurable function on $\Omega(\tau)$.

III. For each triple $\tau \geq \tau_1 \geq \tau_0$, P satisfies the generalized Chapman-Kolmogorov relation,

$$P[\Gamma(\tau)|\omega(\tau_0)] = \int_{\Sigma(\tau_1)} P[\Gamma(\tau)|\omega(\tau_1)]P[d\omega(\tau_1)|\omega(\tau_0)]. \tag{1}$$

This means that if $\Gamma(\tau) = A \times S(\tau)$, where $A \in B(V)$ and $S(\tau) \in B(\tau)$, then $P[\Gamma(\tau)|\omega(\tau_0)]$ is the probability that, given a particle with initial position $x(\tau_0)$ inside τ, in the state ν_0, the particle eventually makes a first passage through some point $x(\tau) \in S(\tau)$ in some state $\nu \in A$. So we can see that $\varkappa[\tau|\omega(\tau_0)] = P[\Sigma(\tau)|\omega(\tau_0)]$ is the total first-passage probability for the

---

*By "state," we understand the set of values of the particle momentum, energy, spin, etc.

particle, given the initial phase $\omega(\tau_0)$, and that $\eta[\tau|\omega(\tau_0)] = 1 - \varkappa[\tau|\omega(\tau_0)]$ is the probability of no passage through τ, given the initial phase $\omega(\tau_0)$, and represents the stopping probability.

We shall generalize even more the kind of process for which we can define the stopping probability by introducing a discontinuous first-passage process[10,11] as the one whose first-passage function satisfies the conditions stated above and the integral equation

$$P[\Gamma(\tau)|\omega(\tau_0)] = P_0[\Gamma(\tau)|\omega(\tau_0)] + \int_{\Omega(\tau)} P[\Gamma(\tau)|\omega]Q[d\omega, \tau|\omega(\tau_0)]. \tag{2}$$

In an abbreviated notation, $P = P_0 + P*Q$, for each pair $\tau \geq \tau_0$, where P_0 and Q satisfy the conditions:

I'. P_0 is a first passage function.

II'. For each $\tau \in \Gamma$, Q is a conditional probability distribution on $B[\Omega(\tau)] \times \Omega(\tau)$.

III'. (a) For each triple $\tau \geq \tau_1 \geq \tau_0$, P_0 and Q satisfy the joint consistency relation

$$Q[\Gamma(\tau), \tau|\omega(\tau_0)] = Q[\Lambda(\tau_1), \tau_1|\omega(\tau_0)] + \int_{\Sigma(\tau_1)} Q[\Lambda(\tau), \tau|\omega(\tau_1)]P_0[d\omega(\tau_1)|\omega(\tau_0)], \tag{3}$$

where $\Lambda(\tau_1) = \Lambda(\tau) \cap \Omega(\tau_1)$.

(b) For each pair $\tau \geq \tau_0$, $\varkappa_0[\tau|\omega(\tau_0)] + \theta[\tau|\omega(\tau_0)] \leq 1$, where $\varkappa_0[\tau|\omega(\tau_0)] = P_0[\Sigma(\tau)|\omega(\tau_0)]$ and $\theta[\tau|\omega(\tau_0)] = Q[\Omega(\tau), \tau|\omega(\tau_0)]$.

The situation now is that we have split the process in two: a process in which the state of the particles is changed in a continuous form, and a process in which the state is changed by jumps. Then, P_0 is a first passage probability with no jumps and Q is the probability of a first jump and consequent state before a first passage through τ. Of course we could consider just a certain kind of jump in Q and include in P_0 any other way of changing the state of the particle. Following this interpretation, $\varkappa_0[\tau|\omega(\tau_0)]$ is the total probability of a first passage through τ with no prior jumps and $\theta[\tau|\omega(\tau_0)]$ is the total probability of a first jump before a first passage through τ. Then $\eta_0[\tau|\omega(\tau_0)] = 1 - \varkappa_0[\tau|\omega(\tau_0)] - \theta[\tau|\omega(\tau_0)]$ is the probability of no jumps and no first passage through τ; and $\varkappa$ and η are now defined from P as before.

From Eq. 2 and the fact that $\eta = 1 - \varkappa$, $\eta_0 = 1 - \varkappa_0 - \theta$, $1*Q = \theta$ and $1 - \eta = 1 - \eta_0 - \theta + (1 - \eta)*Q = 1 - \eta_0 - \eta*Q$, we can see that the stopping probability η is given by the integral equation

$$\eta[\tau\,|\,\omega(\tau_0)] = \eta_0[\tau\,|\,\omega(\tau_0)] + \int_{\Omega(\tau)} \eta(\tau\,|\,\omega)Q[d\omega,\,\tau\,|\,\omega(\tau_0)], \tag{4}$$

or

$$\eta = \eta_0 + \eta*Q. \tag{5}$$

Furthermore, since P satisfies the Chapman-Kolmogorov equation, we have

$$\varkappa[\tau\,|\,\omega(\tau_0)] = \int_{\Sigma(\tau_1)} \varkappa[\tau\,|\,\omega(\tau_1)]P[d\omega(\tau_1)\,|\,\omega(\tau_0)], \qquad \tau \geq \tau_1 \geq \tau_0. \tag{6}$$

Hence, substituting $1 - \eta$ for $\varkappa$ into Eq. 6 yields the consistency relation

$$\eta[\tau\,|\,\omega(\tau_0)] = \eta[\tau_1\,|\,\omega(\tau_0)] + \int_{\Sigma(\tau_1)} \eta[\tau\,|\,\omega(\tau_1)]P[d\omega(\tau_1)\,|\,\omega(\tau_0)], \qquad \tau \geq \tau_1 \geq \tau_0. \tag{7}$$

To discuss the existence and uniqueness of solutions of Eq. 5 satisfying condition 7, we introduce:

$$Q_{n+1} = Q_n*Q, \quad Q_0 = 1, \quad P_{n+1} = P*Q_n,$$

$$\eta_n = \eta_0*Q_n, \quad \theta_n = \theta*Q_{n-1}, \quad \theta_\infty = \lim_{n\to\infty} \theta_n,$$

and notice that, with the interpretations given before, $\eta_n[\tau\,|\,\omega(\tau_0)]$ is the probability of no first passage through τ after exactly n jumps inside τ, and $\theta_\infty[\tau\,|\,\omega(\tau_0)]$ is the probability of an infinite number of jumps before such a first passage.

Now we can state the following:

Theorem. $\eta_R = \sum\limits_{n=0}^{\infty} \eta_n$ is the smallest nonnegative solution of Eq. 5 that satisfies Eq. 7; it is the unique bounded solution of Eq. 5 if and only if $\theta_\infty \equiv 0$.

This theorem has been proved in Ref. 10 for the first-passage probability P. Since η_R is given by the same equation as P (Eq. 5) with the same Q, it only remains to prove that it satisfies the consistency condition Eq. 7. First we can write a relation analogous to Eq. 3 for Q_n in the form

$$Q_n[\Lambda(\tau), \tau \,|\, \omega(\tau_0)] = Q_n[\Lambda(\tau_1), \tau_1 \,|\, \omega(\tau_0)]$$

$$+ \sum_{j=1}^{n} \int_{\Sigma(\tau_1)} Q_j[\Lambda(\tau), \tau \,|\, \omega(\tau_1)] P_{n-j}[d\omega(\tau_1) \,|\, \omega(\tau_0)],$$

$$\tau \geq \tau_1 \geq \tau_0; \qquad n = 1, 2, \ldots . \tag{8}$$

On the other hand, η_0 satisfies

$$\eta_0[\tau \,|\, \omega(\tau_0)] = \eta_0[\tau_1 \,|\, \omega(\tau_0)]$$

$$+ \int_{\Sigma(\tau_1)} \eta_0[\tau \,|\, \omega(\tau_1)] P_0[d\omega(\tau_1) \,|\, \omega(\tau_0)], \qquad \tau \geq \tau_1 \geq \tau_0. \tag{9}$$

Substituting Eqs. 8 and 9 into the equation $\eta_n = \eta_0 * Q_n$ and making use of $P_0 * Q_k = P_k$, we obtain

$$\eta_n[\tau \,|\, \omega(\tau_0)] = \eta_n[\tau_1 \,|\, \omega(\tau_0)] + \sum_{j=0}^{n} \int_{\Sigma(\tau_1)} \eta_j[\tau \,|\, \omega(\tau_1)] P_{n-j}[d\omega(\tau_1) \,|\, \omega(\tau_0)],$$

$$\tau \geq \tau_1 \geq \tau_0. \tag{10}$$

Finally,

$$\eta_R[\tau \,|\, \omega(\tau_0)] = \sum_{n=0}^{\infty} \eta_n[\tau \,|\, \omega(\tau_0)]$$

$$= \sum_{n=0}^{\infty} \left\{ \eta_n[\tau_1 \,|\, \omega(\tau_0)] + \sum_{j=0}^{n} \int_{\Sigma(\tau_1)} \eta_j[\tau \,|\, \omega(\tau_1)] P_{n-j}[d\omega(\tau_1) \,|\, \omega(\tau_0)] \right\}$$

$$= \eta_R[\tau_1 \,|\, \omega(\tau_0)] + \int_{\Sigma(\tau_1)} \eta_R[\tau \,|\, \omega(\tau_1)] P[d\omega(\tau_1) \,|\, \omega(\tau_0)]. \tag{11}$$

The most general solution of Eq. 5, as we shall see, consists of the sum of the terms η_R and θ_∞. If we put $\varkappa_n = \varkappa_0 * Q_n$, then $\theta_{n+1} = \theta * Q_n = (1 - \varkappa_0 - \eta_0) * Q_n = \theta_n - \varkappa_n - \eta_n$, and, by iteration,

$$\theta_{n+1} = 1 - \sum_{j=0}^{n} (\varkappa_j + \eta_j).$$

Since the limit for $n \to \infty$ exists,[11] it follows that

$$\theta_\infty = 1 - \sum_{j=0}^{\infty} (\varkappa_j + \eta_j) = 1 - \varkappa_R - \eta_R,$$

where we put

$$\varkappa_R = \sum_{j=0}^{\infty} \varkappa_j.$$

So we see that $\eta = 1 - \varkappa_R = \eta_R + \theta_\infty$. This means that if $\theta_\infty \equiv 0$ (<u>stable process</u>), the stopping probability is given by $\varkappa_R$, while if $\theta_\infty \neq 0$ (unstable process), the stopping probability receives a contribution θ_∞ involving an infinite number of collisions.

C. Pure Jump Process with Finite Collision Rate

In this section, we shall restrict the process to a pure jump process and assume a finite collision rate. We shall see how the general formulation of Section B above reduces to a well-known backward integro-differential equation.

Let us split the state variable ν in the form $\nu = (\mu, \gamma)$, where μ is the unit vector in the direction of motion of the particle and γ includes the remaining state variables. Then, the position vector of a particle that is initially at x and undergoes no collisions in traveling a length of path s becomes $x + \mu s$.

Now we assume that the probability that a particle at x and in state (μ, γ) suffers a collision while traveling a distance δs is $\lambda(\mu, \gamma, x)\delta s + O(\delta s)$, and the probability of more than one collision is $O(\delta s)$.

Let $\varphi(A | \mu_0, \gamma_0, x_0)$ be the transition probability from the state (μ_0, γ_0) to some state $(\mu, \gamma) \in A$, given that a collision occurred at x_0.

If for any given surface τ, $R(\mu_0, x_0, \tau) = \inf(s | x_0 + \mu_0 s \in \tau)$, then for a pure jump process, we have

$$\eta_0(\tau | \mu_0, \gamma_0, x_0) = \exp\left[- \int_0^{R(\mu_0, x_0, \tau)} \lambda(\mu_0, \gamma_0, x_0 + \mu_0 s) \, ds \right]$$

$$\delta[\tau | x_0 + \mu_0 R(\mu_0, x_0, \tau)] \tag{12}$$

and

$$Q(A \times S, \tau | \mu_0, \gamma_0, x_0) = \int_0^{R(\mu_0, x_0, \tau)} \varphi(A | \mu_0, \gamma_0, x_0 + \mu_0 s) \; \delta(S | x_0 + \mu_0 s)$$

$$\exp\left[-\int_0^s \lambda(\mu_0, \gamma_0, x_0 + \mu_0 \xi) \, d\xi\right] \lambda(\mu_0, \gamma_0, x_0 + \mu_0 s) \, ds, \tag{13}$$

where $A \in B(V)$, $S \in \tau$, $x_0 = x(\tau_0)$, $\tau_0 \leq \tau$, and

$$\delta(C | t) = \begin{cases} 1 \text{ if } t \in C, \\ 0 \text{ if } t \notin C. \end{cases}$$

Substituting Eqs. 12 and 13 into Eq. 5, we obtain

$$\eta(\tau | \mu_0, \gamma_0, x_0) = \exp\left[-\int_0^{R(\mu_0, x_0, \tau)}\right] \lambda(\mu_0, \gamma_0, x_0 + \mu_0 s) \, ds \; \delta[\tau | x_0 + \mu_0 R(\mu_0, x_0, \tau)]$$

$$+ \int_V \int_0^{R(\mu_0, x_0, \tau)} \lambda(\mu, \gamma, x_0 + \mu_0 s) \; \varphi(d\mu d\gamma | \mu_0, \gamma_0, x_0 + \mu_0 s)$$

$$\exp\left[-\int_0^s \lambda(\mu_0, \gamma_0, x_0 + \mu_0 \xi) \, d\xi\right] \lambda(\mu_0, \gamma_0, x_0 + \mu_0 s) \, ds. \tag{14}$$

Using the fact that $R(\mu_0, x_0 + \mu_0 s, \tau) = R(\mu_0, x_0, \tau) - \mu_0 s$ and denoting the spatial derivative of η in the direction of μ_0 by $\mu_0 \cdot (\partial/\partial x_0)\eta$, we finally obtain from Eq. 14 the "backward" integro-differential equation

$$\mu_0 \cdot \frac{\partial}{\partial x_0} \eta(\tau | \mu_0, \gamma_0, x_0) = \lambda(\mu_0, \gamma_0, x_0)\eta(\tau | \mu_0, \gamma_0, x_0)$$

$$- \lambda(\mu_0, \gamma_0, x_0) \int_V \eta(\tau | \mu, \gamma, x_0)\varphi(d\mu d\gamma | \mu_0, \gamma_0, x_0). \tag{15}$$

This equation is valid for any kind of range, and we can obtain the equation for any range by appropriately defining the surfaces τ. For example, to obtain the projected range for a certain direction, we take planes perpendicular to that direction. If, on the other hand, we want the lateral range with respect to a given direction, then we have to take cylinders whose common axis is the given direction.

We now turn to the equation for the distribution of the effective range and concentrate on the space homogeneous process, where λ and φ are independent of x_0. If, furthermore, λ is independent of μ and φ depends only on $\mu_1 \cdot \mu_0 = \cos \theta$ (where θ is the angle between the initial and final directions μ_0 and μ_1), then the equation for η simplifies considerably. If we take the surfaces τ to be planes normal to the path of the particle and introduce the path length s, the term $\mu_0 \cdot \partial/\partial x_0$ of Eq. 15 becomes $-\partial/\partial s$ and

$$\varphi'(d\gamma | \gamma_0) = \int \varphi(d\gamma d\mu | \gamma_0, \mu_0)$$

is independent of μ_0. The backward equation now becomes

$$\frac{\partial}{\partial s} \eta(s | \gamma_0) = -\lambda(\gamma_0) \int [\eta(s | \gamma_0) - \eta(s | \gamma)] \, \varphi'(d\gamma | \gamma_0). \tag{16}$$

D. Effective Range Distribution in Simple Cases

Although the quantity of greater interest from the point of view of applications is the projected range R_p,[12] the effective range is a good approximation in the case of penetration of heavy fast ions when the effect of multiple scattering is reduced.

Furthermore, the equation for the distribution of the effective range is simple enough to be solved exactly for some special forms of the scattering function.

Let us take the energy E as the unique state variable for the penetrating particle and assume that the scattering function $\varphi(dE | E_0)$ has the form

$$\varphi(dE | E_0) = \frac{a(E)}{b(E_0)} \, dE. \tag{17}$$

Then we shall seek the solution of

$$\frac{\partial}{\partial t} \eta_e(t | E_0) = -\lambda(E_0)\eta_e(t | E_0) + \lambda(E_0) \int_{\epsilon}^{E_0} \eta_e(t | E) \frac{a(E)}{b(E_0)} \, dE \tag{18}$$

for arbitrary $\lambda(E_0)$.

Using the Laplace transform

$$\hat{\eta}_e(\alpha | E_0) = \int_0^{\infty} e^{-\alpha t} \eta_e(t | E_0) \, dt = L\{\eta_e\}$$

and the "initial" condition $\eta_e(0|E_0) = 0$, we transform Eq. 18 into

$$b(E_0)[1 + \alpha/\lambda(E_0)]\,\hat{\eta}_e(\alpha|E_0) = \int_\epsilon^{E_0} \hat{\eta}_e(\alpha|E)a(E)\,dE.$$

Differentiating with respect to E_0, we obtain

$$\frac{\delta\varphi}{\delta E_0} = a(E_0)\varphi/\{[1 + \alpha/\lambda(E_0)]\,b(E_0)\},$$

where

$$\varphi = [1 + \alpha/\lambda(E_0)]\,b(E_0)\hat{\eta}_e(\alpha|E_0).$$

After integration, and using the condition $\hat{\eta}_e(\alpha|\epsilon) = 1/\alpha$, we obtain

$$\hat{\eta}_e(\alpha|E_0) = \frac{b(\epsilon)[1 + \alpha/\lambda(\epsilon)]}{\alpha b(E_0)[1 + \alpha/\lambda(E_0)]} \exp\left(\int_\epsilon^{E_0} dE\; a(E)/\{b(E_0)[1 + \alpha/\lambda(E)]\}\right). \qquad (19)$$

Now, since φ must be normalized in such a way that

$$\int_\epsilon^{E_0} \frac{a(E)}{b(E_0)}\,dE = 1,$$

it follows that

$$b(E_0) = \int_\epsilon^{E_0} a(E)\,dE,$$

and therefore $a(E) = db/dE$.

Hence the equation for $\hat{\eta}_e$ becomes

$$\alpha\hat{\eta}_e(\alpha|E_0) = \frac{b(\epsilon)[1 + \alpha/\lambda(\epsilon)]}{b(E_0)[1 + \alpha/\lambda(E_0)]} \exp\left(\int_\epsilon^{E_0} db(E)/\{b(E)[1 + \alpha/\lambda(E)]\}\right). \qquad (20)$$

Expanding the exponential in the right-hand side of Eq. 20 and putting $\theta(t|E_0) = L^{-1}\{\alpha\hat{\eta}_e\}$ for the inverse of $\alpha\hat{\eta}_e$ (this means that θ is the probability density function of the probability distribution $\eta(t|E_0)$), we have

$$\theta(t\,|\,E_0) \;=\; L^{-1}\left\{\frac{b(\epsilon)[1+\alpha/\lambda(\epsilon)]}{b(E_0)[1+\alpha/\lambda(E_0)]}\left[1+\sum_{k=1}^{\infty}\frac{1}{k!}\int_{\epsilon}^{E_0}\cdots\int_{\epsilon}^{E_0}\prod_{j=1}^{k}\frac{db(E_j)}{b(E_j)}\frac{\lambda(E_j)}{\alpha+\lambda(E_j)}\right]\right\}$$

$$=\;\left[L^{-1}\left\{\frac{b(\epsilon)[1+\alpha/\lambda(\epsilon)]}{b(E_0)[1+\alpha/\lambda(E_0)]}\right\}\right]^{*}\left\{\delta(t)+\sum_{k=1}^{\infty}\frac{1}{k!}\int_{\epsilon}^{E_0}\cdots\int_{\epsilon}^{E_0}\prod_{j=1}^{k}\frac{db(E_j)\lambda(E_j)}{b(E_j)}\sum_{i=1}^{k}\frac{\exp[-\lambda(E_i)]}{\prod_{\ell\neq i}^{k}[\lambda(E_\ell)-\lambda(E_i)]}\right\},$$

and finally,

$$\theta(t\,|\,E_0)\;=\;\frac{b(\epsilon)}{b(E_0)}\left[\frac{1}{\lambda(E_0)}-\frac{1}{\lambda(\epsilon)}\right]\exp[-\lambda(E_0)t]\left(1+\sum_{k=1}^{\infty}\frac{1}{k!}\sum_{i=1}^{k}\int_{\epsilon}^{E_0}\cdots\right.$$

$$\left.\int_{\epsilon}^{E_0}\frac{\displaystyle\prod_{j=1}^{k}\lambda(E_j)d[\ell n\,b(E_j)]}{\displaystyle\prod_{\ell\neq i}^{k}[\lambda(E_\ell)-\lambda(E_i)]}\;\frac{1-\exp\{-t[\lambda(E_i)-\lambda(E_0)]\}}{\lambda(E_0)-\lambda(E_i)}\right). \tag{21}$$

The moments of the distribution can be obtained directly from Eq. 20 in the form

$$\langle R_e^k(E_0)\rangle \;=\; (-)^k\left[\frac{\partial^k}{\partial\alpha^k}\,\alpha\hat{\eta}_e(\alpha\,|\,E_0)\right]_{\alpha=0}.$$

The first two are

$$\langle R_e(E_0)\rangle \;=\; \int_{\epsilon}^{E_0}\frac{d[\ell n\,b(E)]}{\lambda(E)}+\left(\frac{1}{\lambda(E_0)}-\frac{1}{\lambda(\epsilon)}\right)$$

and

$$\langle R_e^2(E_0)\rangle \;=\; \langle R_e(E_0)\rangle^2 + 2\int_{\epsilon}^{E_0}\frac{d[\ell n\,b(E)]}{\lambda^2(E)}+\frac{2}{\lambda(E_0)}\left(\frac{1}{\lambda(E_0)}-\frac{1}{\lambda(\epsilon)}\right)$$

$$-\left(\frac{1}{\lambda(E_0)}-\frac{1}{\lambda(\epsilon)}\right)^2.$$

Solutions can be immediately obtained directly from Eq. 20 in some simple cases. The results are presented in a schematic way in Table I.

TABLE I. Stopping Probability in Very Simple Cases

λ	φ	ϵ	$\eta(t\,|\,E_0)$
$1/E$	dE/E_0	0	$1 - (1 + t/E_0)\,e^{-t/E_0}$
$1/E$	$\dfrac{2E\,dE}{E_0^2}$	0	$\displaystyle\int_0^{t/E_0} \frac{\tau^2}{2!}\,e^{-\tau}\,d\tau$
$1/E^{\nu}$	dE/E_0	0	$\dfrac{1}{\Gamma\!\left(\dfrac{1}{\nu}-1\right)} \displaystyle\int_0^{t/E_0^{\nu}} \tau^{1/\nu}e^{-\tau}\,d\tau$ (gamma distribution)

E. Possible Generalizations

The theory developed here is valid for an amorphous substance. In a medium like a crystalline solid, we must take into account collective effects, and the collisions with the atoms of the material will no longer be mutually independent. This causes the process to lose its Markovian character.

However, we could consider as an approximation that the crystal is an amorphous substance in which "strings" and "planes" of atoms are imbedded in a random way. Due to the general definition of a discontinuous first-passage process and to the elasticity of the concept of "jump" in the state of the particle, we can consider that the continuous part η_0 of the stopping probability represents now the solution for the material considered to be amorphous, while the "jump" part of Eq. 5 represents the contribution of the scattering by a "string" and a "plane" of atoms.

The difficulty is to define scattering functions for such events. There are already some studies of scattering by collective systems of atoms; a fairly general account appears in Ref. 13.

III. THE IONIZATION CASCADE

A. Introduction and Summary

A fast charged primary particle passing through an absorber ejects knock-on electrons, each of which, if energetic enough, will ionize further atoms. The theory of such an ionization cascade was developed in a previous paper[14] (referred to henceforth as I). In the present report, we review and extend the relevant parts of I, leading to a numerical computation

of the distribution of numbers of ion-pairs produced by a primary of given energy passing through a homogeneous absorber. We will show that this distribution can be expressed to a good approximation in terms of a universal law, namely, the approximate analytic form for the Landau universal distribution for energy loss by ionization first given in Ref. 15 (referred to henceforth as II).

One striking feature of ionization by fast charged particles is the linear dependence of primary energy loss on the number of ion-pairs produced, the most probable energy loss per ion-pair being independent of the primary energy, and varying little with the nature of the absorber (of the order of 35 eV per ion-pair). In this report, we obtain an expression for the mean number $\overline{N}(W)$ of ion-pairs conditional on a loss of energy W by the primary. It is found that $\overline{N}(W)$ is independent of the initial energy. Furthermore, if E_p is the most probable primary energy loss, then a numerical computation shows that $\overline{N}(E_p)$ varies linearly with E_p, while $(d\overline{N}/dE_p)^{-1}$ yields a value for the energy loss per ion-pair in fairly good agreement with the experimental results. (Qualitative explanations of this phenomenon have been advanced in Refs. 16-18.)

B. Theory of the Ionization Cascade

In this section, we review and extend the relevant parts of I. Let $p_n(u|E;t)\,du$ be the probability that a primary of initial energy E produces exactly n cascade electrons while losing energy between u and u + du in time t. The cascade process may then be characterized by the generating function

$$\Psi(z, \lambda \,|\, E;t) = \sum_{n=0}^{\infty} z^n \int_0^E e^{-\lambda U} p_n(U\,|\,E;t)\,dU. \tag{22}$$

Setting $z \equiv 0$ in Ψ yields the Laplace transform of the primary energy-loss distribution $\rho(u\,|\,E;t)$,

$$\hat{\rho}(\lambda \,|\, E;t) = \int_0^E e^{-\lambda U} \rho(U\,|\,E;t)\,dU = \Psi(0, \lambda\,|\,E;t). \tag{23}$$

Setting $\lambda = 0$, we obtain the probability generating function (briefly, p.g.f.) for the cascade number distribution

$$G_p(z\,|\,E;t) = \sum_{n=0}^{\infty} z^n P_n(E;t) = \Psi(z, 0\,|\,E;t), \tag{24}$$

where

$$P_n(E;t) = \int_0^E p_n(U|E;t) \, dU$$

is the probability of a total of exactly n electrons in the cascade.

For a fast primary, the knock-on electrons are emitted overwhelmingly with energies that are small compared to the primary energy E, and the secondary cascades each such knock-on initiates are small and terminate near the path of the primary. Hence, to a good approximation, we may allow that all such secondary cascades have terminated in the calculation of Ψ. Let $q_n(U)$ be the probability of exactly n electrons in such a terminated cascade initiated by a knock-on of energy U, and let

$$g(z|U) = \sum_{n=1}^{\infty} z^n q_n(U)$$

be the corresponding p.g.f. Let $\Pi_p(U|E)$ be the differential collision rate (per unit time) for primary energy loss, and let us assume that the primary ionizes only when it loses energy $U \geq I$, where I is a mean ionization potential for the absorber atoms, thereby initiating a secondary cascade with initial knock-on energy U - I. Then Ψ satisfies the "backward" integro-differential equation

$$\frac{\partial}{\partial t} \Psi(E;t) = \int_0^E \{\Psi(E - U;t) \, g(U - I) - \Psi(E;t)\} \, \Pi_p(U|E) \, dU, \tag{25}$$

where we have suppressed indication of the dependence of Ψ and g on z and λ and conventionally set g(U - I) = 1 for $U \leq I$.

If E is very large compared to the most probable energy loss, we can, to a good approximation, substitute $\Psi(E)e^{-\lambda U}$ for $\Psi(E - U)$ in Eq. 25. We obtain

$$\frac{\partial}{\partial t} \Psi(E;t) = \Psi(E;t) \int_0^E [e^{-\lambda U} g(U - I) - 1] \, \Pi_p(U|E) \, dU, \tag{26}$$

whose solution [with initial condition $\Psi(E;0) \equiv 1$] is conveniently written in the form

$$\Psi(z, \lambda \,|\, E; t) = \exp\left\{\alpha_p(E)t \int_0^E [e^{-\lambda U} g(z\,|\,U - I) - 1] \, \varphi_p(U\,|\,E) \, dU\right\}, \quad (27)$$

where $\alpha_p(E) = \displaystyle\int_0^E \Pi_p(U\,|\,E) \, dU$ and $\varphi_p = \Pi_p/\alpha_p$. Then (see II and I),

$$\hat{\rho}(\lambda \,|\, E; t) = \exp\left[\alpha_p(E)t \int_0^E (e^{-\lambda U} - 1) \, \varphi_p(U\,|\,E) \, dU\right] \quad (28)$$

and

$$G_p(z\,|\,E; t) = \exp\left[\alpha_p(E)t \sum_{n=1}^{\infty} (z^n - 1) \, Q_n(E)\right], \quad (29)$$

where

$$Q_n(E) = \int_I^E q_n(U - I) \, \varphi_p(U\,|\,E) \, dU.$$

To evaluate $g(z\,|\,E)$, we assume again that a cascade electron ionizes only when it loses energy $U \geq I$ (the mean ionization potential), thereby ejecting a further cascade electron of energy $U - I$. Let $\Pi(U\,|\,E)$ be the differential collision rate for energy loss of an electron of energy E, and let $\chi(W\,|\,E; t)$ be the final energy probability density with no ionizing collisions for an electron of initial energy E in time t. Then χ satisfies the "backward" equation

$$\left[\frac{\partial}{\partial t} + \alpha(E)\right] \chi(W\,|\,E; t) = \int_0^I \chi(W\,|\,E - U; t) \, \Pi(U\,|\,E) \, dU, \quad (30)$$

where $\alpha(E) = \displaystyle\int_0^E \Pi(U\,|\,E) \, dU$, while the p.g.f. $G(z\,|\,E; t)$ for the number of electrons in a secondary cascade initiated by a knock-on of energy E in time t satisfies the integral equation (cf. I)

$$G(z\,|\,E; t) = z\chi_t(E) + \int_0^t ds \int_I^E dW \int_I^W dU \, G(z\,|\,W - U; t - s) \, G(z\,|\,U - I; t - s)$$

$$\chi(W\,|\,E; s) \Pi(U\,|\,W), \quad (31)$$

where

$$\chi_t(E) = \int_0^E \chi(W|E;t)\, dW.$$

Only nonionizing collisions contribute to the change with time of χ. In any time interval t of interest, we can expect that the number of such collisions will be very large, while the energy loss in each collision will be very small as long as $E \gg I$; hence a "diffusion approximation" to Eq. 30 is legitimate. Expanding the integrand on the right-hand side of Eq. 30 in a Taylor series and neglecting terms of third order, we obtain the diffusion equation

$$\left[\frac{\partial}{\partial t} + \alpha_i(E) + a(E) \frac{\partial}{\partial E} - \tfrac{1}{2} b(E) \frac{\partial^2}{\partial E^2} \right] \chi(W|E;t) = 0, \tag{32}$$

where

$$\alpha_i(E) = \int_I^E \Pi(U|E)\, dU; \quad a(E) = \int_0^I U\Pi(U|E)\, dU; \quad b(E) = \int_0^I U^2\Pi(U|E)\, dU.$$

A "zero-order" approximation is to neglect loss of energy by nonionizing collisions; i.e., take

$$\chi(W|E;t) = \delta(W-E)\, e^{-\alpha_i(E)t}. \tag{33}$$

If we set $b \equiv 0$ in Eq. 32, we obtain the "deterministic" solution

$$\chi(W|E;t) = \delta[W - \mathscr{E}(E;t)] \exp\left[- \int_{\mathscr{E}(E;t)}^E a^{-1}(U)\alpha_i(U)\, dU \right], \tag{34}$$

where the final energy $\mathscr{E}(E;t)$ is defined implicitly by

$$t = \int_{\mathscr{E}(E;t)}^E a^{-1}(U)\, dU.$$

An approximate Gaussian solution to Eq. 32, namely

$$\chi(W|E;t) = [2\pi\sigma^2(E;t)]^{-1/2} \exp\{-[E - W - m(E;t)]^2/2\sigma^2(E;t) - \lambda(E;t)\}, \tag{35}$$

where

$$\lambda(E;t) = \int_0^t \alpha_i[\mathscr{E}(E;s)]\, ds,$$

$$m(E;t) = \int_0^t a[\mathcal{E}(E;s)]\, ds,$$

and

$$\sigma^2(E;t) = \int_0^t b[\mathcal{E}(E;s)]\, ds,$$

is obtained via the "forward" equation

$$\left[\frac{\partial}{\partial t} + \alpha_i(W) - \frac{\partial}{\partial W}\, a(W) - \frac{1}{2}\frac{\partial^2}{\partial W^2}\, b(W)\right]\chi(W|E;t) = 0 \tag{36}$$

adjoint to Eq. 32 by substituting $\mathcal{E}(E;t)$ for W in the expressions for α_i, a, and b; note that the right-hand side of Eq. 35 converges to that of Eq. 34 when $\sigma^2 \to 0$.

A good approximation to the p.g.f $g(z|E)$ of the terminated secondary cascade is now obtained by setting $g(z|E) = G(z|E;T)$, where T is the time required for the "deterministic" final energy $\mathcal{E}(E;t)$ to vanish; i.e.,

$$T = \int_0^E a^{-1}(U)\, dU.$$

Substituting in Eq. 31, we obtain an integral equation for g,

$$g(z|E) = z\chi_T(E) + \int_I^E dW \int_I^W dU\, g(z|W-U)\, g(z|U-I)\, K(U,W,E), \tag{37}$$

where

$$K(U,W,E) = \Pi(U|W)\int_0^T \chi(W|E;t)\, dt.$$

C. Computation of the Cascade Number Distributions

We begin by computing the secondary-cascade number distribution. Clearly, $g(z|E) = z$ when $0 \le E < I$. It follows by induction (cf. I) that in the energy range $(k-1)I \le E < kI$,

$$g(z|E) = \sum_1^k z^j q_j(E)$$

(i.e., $q_j(E) = 0$ for $j > k$), and that the integrand on the right-hand side of Eq. 37 involves only products $g(z|W)$ for values of $W < (k-1)I$: This yields

an iterative scheme for the computation of $g(z|E)$, and hence of the $q_k(E)$, in successive energy intervals of length I. Furthermore, in the interval $(k-1) I \leq E < kI$, we have

$$\sum_1^k q_j(E) = 1$$

and hence need only compute $q_1, \ldots, q_{k-1}$. Substituting the polynomial expansion of $g(z|E)$ into Eq. 37, we find that

$$q_1(E) = \chi_T(E) \text{ for all } E \geq I \tag{38}$$

and obtain the iterative relation

$$q_k(E) = \int_I^E dW \int_I^W dU \sum_{j=1}^{k-1} q_j(W - U) q_{k-j-1}(U - I) K(U, W, E)$$

$$\text{for } E \geq kI, \ k = 2, 3, \ldots . \tag{39}$$

The electrons in the secondary cascade are predominantly of low energy, and the energy loss at each collision is predominantly in the neighborhood of the ionization potential. No simple expression for the differential cross section $\sigma(U|E)$ for energy loss U is available in this region, but it is known (see Eq. 27) that it exhibits a single maximum at $U = I$ and approaches rapidly to the Rutherford cross section σ_R for increasing U; hence we use a phenomenological "resonance" expression for σ (cf. II)

$$\sigma(U|E) dU = \frac{B}{E} \frac{dU}{(U - I)^2 + \Gamma^2}, \tag{40}$$

which tends to the Rutherford cross section $\sigma_R dU = BdU/EU^2$ with increasing U. ($B = \pi Z z^2 e^4$, where Z is the atomic number of the absorber atoms, e is the charge of the electron, and ze is the charge of the impinging particle.) The half-width Γ of the resonance curve is evaluated by comparing with experimental values the calculated value of the primary ionization rate, which is proportional to

$$\int_I^E \sigma \, dU,$$

and hence is approximately Γ^{-1}. The differential collision rate is then $M = Nv\sigma$, where N is the number density of scattering centers and v is the primary velocity.

Substituting this expression for Π in the expressions obtained in Section B above, we can compute the functions $K(U, W, E)$ and $\chi_T(E) = q_1(E)$, and consequently compute the probabilities $q_k(E)$ for $k \geq 2$ by the iteration relation (Eq. 39).

To evaluate the primary cascade p.g.f. $G_p(z|E;t)$ given by Eq. 29, we need the probabilities

$$Q_k(E) = \int_I^E q_k(U - I) \, \varphi_p(U|E) \, dU; \quad k = 1, 2, 3, \ldots, \tag{41}$$

and hence the primary energy-loss distribution at each collision φ_p. For a fast primary, where $E \gg I$, we can, to a good approximation, use the Rutherford cross section σ_R and replace the upper limit of integration E by ∞; thus we can take $\varphi_p(u) \, du = I \, du/u^2$ (cf. II). Substituting in Eq. 41 and changing variables to $\epsilon = U/I$, we find that the Q_k becomes

$$Q_k = \int_1^\infty q_k[I(\epsilon - 1)] \frac{d\epsilon}{\epsilon^2}; \quad k = 1, 2, \ldots,$$

which is independent of E.

Turning to Eq. 29 for the primary cascade p.g.f. $G_p(z|E;t)$, we see that in the present approximation, G_p and hence the number probabilities P_n depend on E and t only through the product $\alpha_p(E)t = \tau(E, t)$, which is the mean number of collisions experienced by the primary particle in time t, or passing through an absorber of thickness $x = vt$, where v is the velocity of the primary. Changing variable to τ, and further setting $z = e^{-\beta}$, we obtain the Laplace transform of the primary-cascade number distribution

$$M(\beta, \tau) = G\left(e^{-\beta} \middle| E; \frac{\tau}{\alpha_p(E)}\right) = \sum_{n=0}^\infty e^{-n\beta} P_n(\tau) = e^{\tau R(\beta)}, \tag{42}$$

where

$$R(\beta) = \sum_{k=1}^\infty (e^{-k\beta} - 1) \, Q_k.$$

Let $N(\tau)$ stand for the total number of electrons in the primary cascade after an average of τ primary collisions; i.e., $N(\tau)$ is the random variable with distribution $P_n(\tau) = \text{Probability}[N(\tau) = n]$. For $\tau > 50$, the most probable value $N_p(\tau)$ of N is large, and the distribution

of N is sharply peaked on N_p. For these reasons, we can approximate $P_n(\tau)$ by a continuous distribution $P(\nu, \tau)$ obtained by the first saddle point method applied to the formal inversion of $M(\beta, \tau)$ (cf. II)

$$P(\nu, \tau) = \frac{1}{2\pi i} \int_{c-i\infty}^{c+i\infty} \exp[\tau R(z) + z\nu] \, dz \simeq a^{-1}[2\pi \tau R''(\beta_\nu)]^{-1/2}$$

$$\exp\{\tau[R(\beta_\nu) - \beta_\nu R'(\beta_\nu)]\}, \tag{43}$$

where β_ν is determined implicitly by the relation $\nu = -\tau R'(\beta_\nu)$, while

$$a = -(2\pi\tau)^{-1/2} \int_{\beta_0}^{\beta_\infty} \sqrt{R''(\beta)} \, \exp\{\tau[R(\beta) - \beta R'(\beta)]\} \, d\beta + \tfrac{1}{2} P_0(\tau)$$

is a normalization constant.

A program was written to implement the computations described above on the CDC 3600. The results are shown in Figs. 2-5. Figure 2 shows the probabilities $q_1(E)$, ..., $q_4(E)$ as functions of E, computed for an ionization potential $I = 14.9$ eV and half-width (of the resonance curve) $\Gamma = 6.26$ eV. The probabilities Q_k shown in Fig. 3, converge rapidly to the sequence $c/(k^2 + 1)$, where $c = 0.56$ is a normalization constant. Furthermore, computations showed that the probabilities $q_k(E)$, if plotted as functions of E/I, and hence the distributions Q_k, are not at all sensitive to the value chosen for I in the relevant range of 10-50 eV, while Γ varies little between absorbers. Hence the distributions shown in Figs. 2 and 3 may be considered as universal, i.e., independent of the absorber, thus confirming the results in II. (The values obtained here are somewhat different from those given in II, mainly owing to the fact that loss of energy by nonionizing collisions has been taken into account.)
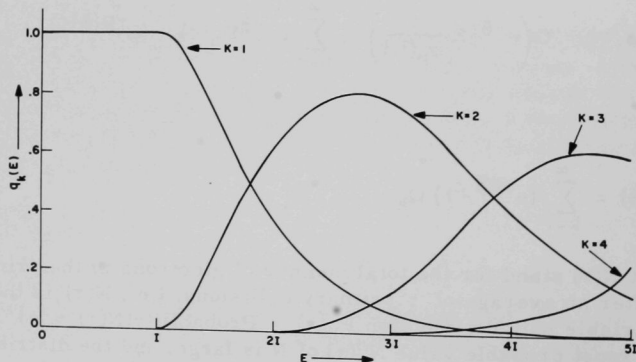
Fig. 2. Probabilities $q_k(E)$. ANL Neg. No. 145-1264.
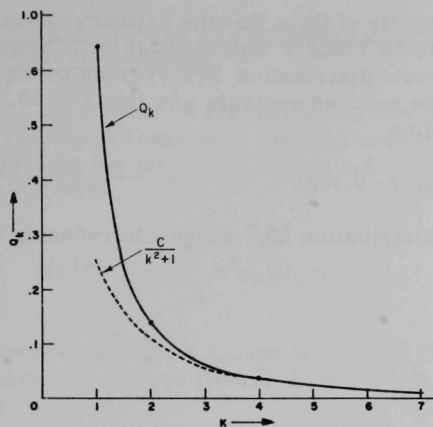
Fig. 3

Probabilities Q_k and $c/(k^2 + 1)$ Law.
ANL Neg. No. 145-1265 Rev. 1.

Fig. 4

Distribution $P(\nu,\tau)$ Given by Eq. 43.
ANL Neg. No. 145-1263.
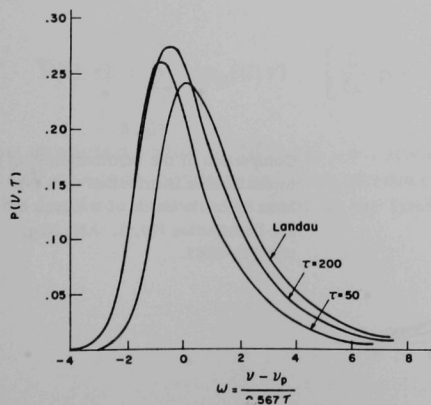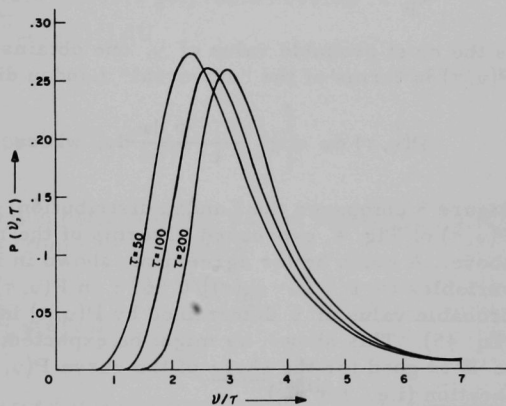
Fig. 5

Comparison of the Distribution $P(\nu,\tau)$
of Fig. 4 to the Landau Distribution.
ANL Neg. No. 145-1270 Rev. 1.

It follows from the universality of Q_n's that the primary cascade number distribution $P_n(\tau)$ depends on I and Γ only through τ. The results of the computation of the approximate distribution $P(\nu, \tau)$ given by Eq. 43 are shown in Fig. 4 in terms of the reduced variable ν/τ for $\tau = 50, 100$, and 200. An approximate expression

$$R(\beta) = -0.413\,\beta + 0.611\,(\log \beta - 0.328) \tag{44}$$

is obtained as in II but using the distribution $\{Q_k\}$ above. Introducing in Eq. 43 the reduced variable

$$\omega = \frac{\nu - \nu_p}{c\tau} = \frac{\nu - \nu_p}{0.567\,\tau},$$

where

$$\nu_p = \tau[0.413 + 0.567\,(\log 1.124\,\tau - 0.672)] \tag{45}$$

is the most probable value of ν, one obtains (again as in II) the distribution $P(\nu, \tau)$ in terms of the "universal" Landau distribution $\chi_L(\omega)$; i.e.,

$$P(\nu, \tau)\,d\nu = \chi_L \frac{\nu - \nu_p}{c\tau} \frac{d\omega}{d\nu}\,d\nu, \text{ where } \chi_L(\omega) = (2\pi)^{-1/2} e^{-1/2(\omega + e^{-\omega})}.$$

Figure 5 compares the Landau distribution $\chi_L(\omega)$ with the distributions $P(\nu, \tau)$ of Fig. 4, expressed in terms of the reduced variable ω defined above. A much better agreement, shown in Fig. 6, is obtained if we change variables to $\omega = [\nu - \nu_p'(\tau)]/0.567\,\tau$ in $P(\nu, \tau)$, where $\nu_p'(\tau)$ is the most probable value of ν determined by $P(\nu, \tau)$ instead of the approximate value (Eq. 45). This shows, as might be expected, that the approximation (Eq. 44) to R is good for the shape of the curve $P(\nu, \tau)$, but rather poor for its location (i.e., for ν_p).
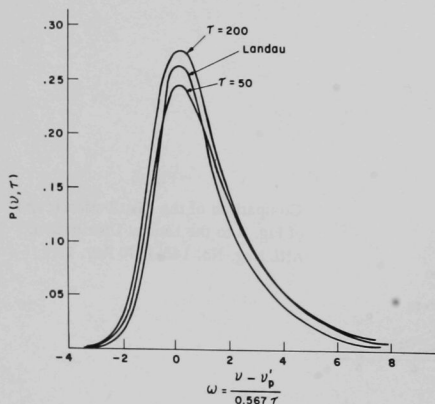
Fig. 6

Comparison of the Distribution $P(\nu,\tau)$ to the Landau Distribution with the Most Probable Value of ν Given by the Distribution $P(\nu,\tau)$. ANL Neg. No. 145-1267.

D. Relation between Primary Energy Loss and Number of Ion-Pairs in Primary Cascades

Let $N(U, \tau)$ be the number of ion-pairs produced by a primary suffering an average of τ ionizing collisions conditional on a primary energy loss (by ionization) U, let $p_n(U, \tau)$ be the distribution of this random variable with

$$\psi(z \mid U; \tau) = \sum_{n=0}^{\infty} z^n p_n(U, \tau)$$

the corresponding p.g.f., and let $\rho(U \mid E; \tau)$ be the probability density for the primary energy loss (where E is as before the initial primary energy). Then

$$\Psi(z, \lambda \mid E; \tau) = \int_0^E \psi(z \mid U; \tau) e^{-\lambda U} \rho(U \mid E; \tau) \, dU$$

$$= \exp\left\{ \tau \int_0^E [e^{-\lambda U} g(z \mid U - I) - 1] \, \varphi_p(U \mid E) \, dU \right\},$$

where Ψ is the generating function defined in Eq. 22 and satisfying Eq. 27, and we have changed variables from t to $\tau = \alpha_p(E)t$. Let

$$\bar{n}(U) = \sum_1^{\infty} n q_n(U) = \left[\frac{\partial}{\partial z} g(z \mid U) \right]_{z=1}$$

be the average number of electrons in a "terminated" secondary cascade, and let

$$\overline{N}(U; \tau) = \sum_1^{\infty} n p_n(U; \tau) = \left[\frac{\partial}{\partial z} \psi(z \mid U; \tau) \right]_{z=1}$$

be the expected value of $N(U; \tau)$, i.e., mean number of ion-pairs in the primary cascade conditional on a primary energy loss U. Using Eq. 23 for the Laplace transform $\hat{\rho}$ of ρ, we find that

$$\left[\frac{\partial}{\partial z}\Psi(z,\lambda\,|\,E;\tau)\right]_{z=1} = \int_0^E \left[\frac{\partial}{\partial z}\psi(z\,|\,U;\tau)\right]_{z=1} e^{-\lambda U}\rho(U\,|\,E;\tau)\,dU$$

$$= \int_0^E \overline{N}(U;\tau)e^{-\lambda U}\rho(U\,|\,E;\tau)\,dU$$

$$= \left\{\tau\int_0^E \left[\frac{\partial}{\partial z}g(z\,|\,U-I)\right]_{z=1} e^{-\lambda U}\varphi_p(U\,|\,E)\,dU\right\}\exp\left[\tau\int_0^E (e^{\lambda U'}-1)\,\varphi_p(U'\,|\,E)\,dU\right]$$

$$= \left[\tau\int_0^E \overline{n}(U-I)\,e^{-\lambda U}\varphi_p(U\,|\,E)\,dU\right]\hat{\rho}(\lambda\,|\,E;\tau);$$

i.e., the Laplace transform of $\overline{N}(U;\tau)\rho(U\,|\,E;\tau)$ is equal to the product of the Laplace transforms of ρ and of $\overline{n}(U-I)\,\varphi_p(U\,|\,E)$. Hence,

$$\overline{N}(W;\tau)\rho(W\,|\,E;\tau) = \tau\int_I^W \rho(W-U\,|\,E;\tau)\,\overline{n}(U-I)\,\varphi_p(U\,|\,E)\,dU$$

$$= \tau\int_0^{W-I} \overline{n}(W-U-I)\,\varphi_p(W-U\,|\,E)\,\rho(U\,|\,E;\tau)\,dU. \qquad (46)$$

Note that $\overline{n}(U) = 0$ when $U < I$. Hence, we take the lower limit of integration to be I instead of 0 in the first expression above, and the upper limit to be $W - I$ in the second expression.

Changing variables to $\omega = (W-E_p)/\tau E_0$, $\eta = (U-E_p)/\tau E_0$, where E_0 is the minimum transferable energy in a primary collision and E_p is the most probable total primary energy loss, transforms $\rho(W\,|\,E;\tau)\,dW$ into the "universal" Landau distribution $\chi_L(\omega)\,d\omega$ (see II), while $\varphi_p(U)\,dU = E_0\,dU/U^2$ becomes $\tau\,d\eta/(\eta+\eta_p)^2$, where $\eta_p = E_p/\tau E_0$. Hence, writing $\eta_I = I/\tau E_0$, we obtain

$$N(\omega) = \overline{N}[\tau E_0(\omega+\eta_p);\tau] = \chi_L^{-1}(\omega)\int_{-\eta_p+\eta_I}^{\omega} \chi_L(\omega-\eta)\,\overline{n}[\tau E_0(\eta+\eta_p-\eta_I)]\frac{d\eta}{(\eta+\eta_p)^2}$$

$$= \chi_L^{-1}(\omega)\int_{-\eta_p}^{\omega-\eta_I} \chi_L(\eta)\overline{n}[\tau E_0(\omega-\eta-\eta_I)]\frac{d\eta}{(\omega-\eta)^2}. \qquad (47)$$

Hence the expression relating the mean number of ion-pairs $\overline{N}$ to the most probable energy loss E_p (see the last paragraph in Section A above and Fig. 7) is [using the fact that $\chi_L(0) = (2\pi e)^{-1/2}$]
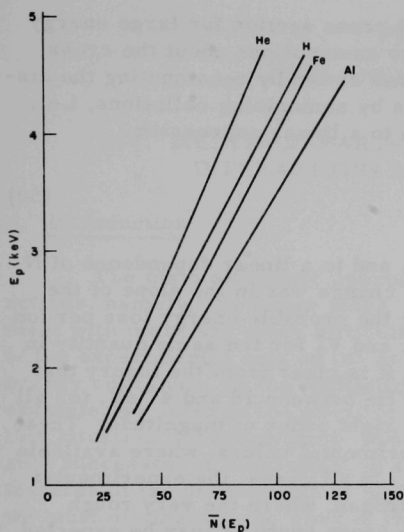
Fig. 7

$\overline{N}(E_p)$ for Several Substances.
ANL Neg. No. 145-1269 Rev. 1.

$$\overline{N}(E_p; \tau) = N(0)$$

$$= (2\pi e)^{1/2} \int_{-\eta_p}^{-\eta_I} \chi_L(\eta)\overline{n}[-\tau E_0(\eta + \eta_I)] \frac{d\eta}{\eta^2}. \quad (48)$$

For $\tau \geq 50$, we can take

$$\eta_p = \frac{E_p}{\tau E_0} \simeq \log 2\tau - c,$$

where $c = 0.577$ is the Euler constant, as a sufficient approximation to the most probable energy loss (see II). The secondary-cascade mean number $\overline{n}(U)$ was computed using the probabilities $q_k(U)$ shown in Fig. 2. Clearly, $\overline{n}(U) = 1$ for $U \leq I$; for $U > I$, $\overline{n}$ varies very nearly linearly with U and can be approximated by (see Fig. 8)

$$\overline{n}(U) = \sum_1^\infty kq_k(U) = 1 + 0.28\left(\frac{U}{I} - 1\right). \quad (49)$$
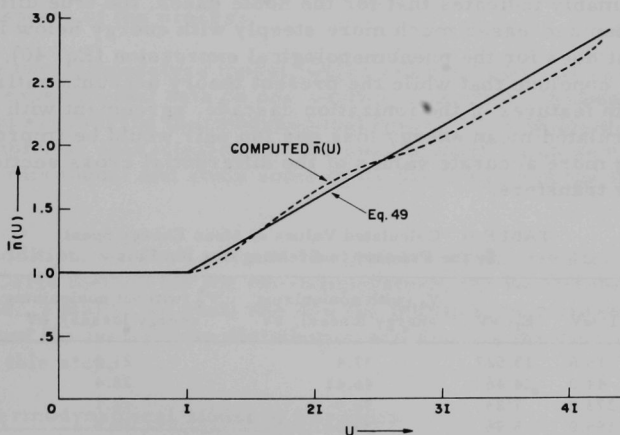
Fig. 8. Computed $\overline{n}(U)$ and Approximation to $\overline{n}(U)$ Given by Eq. 49. ANL Neg. No. 145-1271 Rev. 1.

The function $\overline{N}(E_p; \tau)$ was computed, using Eq. 49 for several absorbers, taking I to be the mean and E_0 the minimum ionizing potentials. The dependence of $\overline{N}$ on E_p is in all cases very nearly linear, as shown in Fig. 7. This result appears to depend essentially on the cascade mechanism

and the E^{-2} dependence of the differential cross section for large energy transfers: it is remarkably insensitive to assumptions about the cross section for low energy transfers. This was shown by recomputing the distributions $q_k(U)$ assuming no energy loss by nonionizing collisions, i.e., adopting Eq. 33 for χ; this led once again to a linear expression

$$\overline{n}(U) = 1 + 0.75\left(\frac{U}{I} - 1\right) \tag{50}$$

for the secondary cascade mean number, and to a linear dependence of $\overline{N}$ on E_p for the same substances: the only change was in the slope of the line. If we let $V_0 = (d\overline{N}/dE_p)^{-1}$ stand for the probable energy loss per ion pair in the first case ($\overline{n}$ given by Eq. 49), and V_0^* for the same quantity in the second case ($\overline{n}$ given by Eq. 50), then it is clear from the theory that $V_0 > V_0^*$, and it was found that V_0 and V_0^* lie between 18 and 47 eV, for all the substances examined, which is of the right order of magnitude. These results and the comparison with the experimental values, where available (from Ref. 20), are displayed in Table II. In all cases, the experimental values lie between V_0 and V_0^*; for the hydrogen, where the very rough assumptions we have made regarding the cross sections may be expected to hold best, one does in fact find an experimental value of 36.3 eV per ion pair very close to the calculated $V_0 = 37.4$ eV per ion pair. The agreement deteriorates for the noble gases with increasing atomic number; for helium, it is still near to the calculated V_0, while for argon, it lies nearer to V_0^*. This presumably indicates that for the noble gases, the true differential cross section decreases much more steeply with energy below its maximum than it does for the phenomenological expression (Eq. 40). We may reasonably conclude that while the present theory accounts satisfactorily for the main features of the ionization cascade, agreement with experiment for the calculated mean energy loss per ion pair would be improved by introducing more accurate values of the differential cross sections for low-energy transfers.

TABLE II. Calculated Values of Mean Energy Spent
by the Primary in Creating One Ion Pair

Substance	I, eV	E_0, eV	V_0 (with nonionizing energy losses), eV	V_0^* (without nonionizing energy losses), eV	V_0 (exper), eV
H	15.6	13.527	37.4	21.2	36.3
He	44.0	24.46	46.42	28.4	42.3
Fe	273.0	7.83	38.0	22.1	-
Al	155.0	5.96	33.0	18.5	-
Ne	95.6	21.47	49.8	28.8	36.6
Ar	305.0	15.68	38.5	21.9	26.4

PART TWO

HIGH-ENERGY PHENOMENA

IV. MULTIPLE-PARTICLE PRODUCTION IN STRONG INTERACTIONS AT VERY HIGH ENERGY

A. Introduction

The main axiomatic approaches to the description of strong interactions, namely, the Regge poles, the quantum field, and quark theories, meet with more and more difficulties in providing a quantitative account of the experimental data on the multiple production of particles in high-energy collisions, as the multiplicity of secondaries increases. As an example, we refer to the effort of Caneschi and Pignotti.[21] In contrast to this situation, thermodynamic and hydrodynamic models have been reasonably successful in describing, in a quantitative way, several (though not all) features of the phenomenon at higher and higher multiplicities. In this area, we must distinguish the work of Heisenberg,[22] Landau,[23] and his followers,[24] in the development of the hydrodynamic theory, and Koppe,[25] Fermi,[26] and Hagedorn[27-29] in the development of the thermodynamic theory.

In addition, there are some purely phenomenological models like the CKP,[30] the two-fireball,[31,32] and the multifireball[33] models, which also account for some aspects of the process.

The two-temperature model, which has been quite successful in describing experimental data on one-particle momentum distributions, has been developed from the thermodynamical theory[34,35] with the incorporation of some empirical characteristics. We shall analyze some new interesting features of this model and study some of its predictions in the light of other models.

In addition, we shall present the inelasticity distribution obtained by the Monte Carlo method for the two-temperature, the two-fireball, and the CKP models. Finally, we shall see how the multiplicity distribution can be obtained from the inelasticity distribution and discuss the difficulties involved in this step.

B. The Thermodynamical Model of Hagedorn

Hagedorn[27-29] has developed a statistical thermodynamics model, which includes barionic number conservation, and applies to the situation created when two strongly interacting particles (hadrons) collide at very high energy.

In such a situation, we have a very big number of particles confined in a small volume (fireball) for a time long enough for the strong interactions to establish an equilibrium between all their possible states and resonances. However, we only distinguish one "particle" from another by its degree of excitation. This led Hagedorn to define a fireball as:

"a statistical equilibrium of an undetermined number of all kinds of fireballs, each of which, in turn is considered to be a statistical equilibrium of an undetermined number of all kinds of fireballs, each of which, in turn is considered to be...[ad infinitum]." (P)

This postulate generates a special kind of thermodynamics.

If $\rho(m)$ dm is the density of states of mass of the secondary fireballs and $\sigma(E)$ dE is the density of energy states of the principal fireball, the partition function of the system can be expressed either as

$$Z = \exp\left[\int_0^\infty \rho(m)F(m, T) \, dm\right]$$

with a known function $F(m, T)$, or as

$$Z = \int_0^\infty \sigma(E)e^{-E/T} \, dE.$$

The postulate (P) implies that the functions $\rho(m)$ and $\sigma(E)$ must have the same behavior as $m \to \infty$. Hagedorn shows that we can require at most that

$$\frac{\log [\rho(m)]}{\log [\sigma(m)]} \to 1 \text{ as } m \to \infty.$$

That is to say, the entropies become the same, and this conditions leads to

$$\rho(m) \to \frac{\text{const}}{m^{5/2}} e^{m/T_0} \text{ as } m \to \infty. \tag{51}$$

Veneziano[36] pointed out that this behavior of the mass spectrum of hadrons can also be predicted starting from a completely different point of view (which is a remarkable coincidence). If the partition function diverges for all values of the temperature $T > T_0$, then this model predicts a maximum temperature $T_0 \sim 160$ MeV for all stable hadronic matter. In other words, T_0 is the boiling temperature for hadronic matter. So, no matter how high the incident energy of a strongly interacting particle is, strong interactions will "control" it so that when T_0 is reached the principal fireball will "boil off" particles, which in turn can produce other particles, and so on.

The occupation number can be calculated as from the partition function

$$f_k(\epsilon, T) = \frac{z_k V}{(2\pi)^3}\left\{\exp\left[\frac{1}{T}(p^2 + m_k^2)^{1/2}\right] \mp 1\right\}^{-1} \tag{52}$$

$(-)$ for bosons

$(+)$ for fermions,

where z_k is the spin-isospin multiplicity of particle "k" and V is the hadronic interaction volume.

As the thermodynamic equilibrium is reached in the reference frame in which the principal fireball is at rest (RFB), kinematics is added to the model by ascribing a collective velocity distribution to it in such a way that the velocity is higher where the temperature is lower. Thus, more peripheral particles are produced with higher velocity.

In the Hagedorn theory, the collective velocity distribution is fitted to obtain good agreement with experimental data by means of two velocity distributions, one for "newly created" particles and one for "through-going" particles.

C. The Two-temperature Model

Starting from the assumption that the transversal momentum $p_{\perp}^*$ and the longitudinal momentum p_{ℓ}^* in the center-of-mass system (CMS) are independent random variables (this is a quite realistic assumption[37]), Wayland and Bowen[34] proposed a model in which "two thermodynamical equilibria" are established in the CMS with two characteristic temperatures T and T_0, and then obtained the distributions for $p_{\perp}^*$ and p_{ℓ}^* from the occupation number (Eq. 52) by integration. At high incident energy, these distributions take the forms

$$W_{\perp}(p_{\perp}^*)\, dp_{\perp}^* = \frac{p_{\perp}^* \mu_2^*}{T_0 m^2 c^2}\, \frac{K_1(\mu_2^*/T_0)}{K_2(mc^2/T_0)}\, dp_{\perp}^*$$

and

$$W_{11}(p_{\ell}^*)\, dp_{\ell}^* = \frac{T}{m^2 c^3}\, \frac{\exp(-\mu_1^*/T)(1 + \mu_1^*/T)}{K_2(mc^2/T)}\, dp_{\ell}^*,$$

$$\tag{53}$$

where

$$\mu_1^{*2} = p_{\ell}^{*2} + m^2$$

and

T_0 is taken as a fitting parameter, and T depends upon the total center-of-mass energy through a second parameter. The fitting of this model to one-particle momentum distributions can be seen in Ref. 35. Efforts have been made[38] to reinterpret the two-temperature model as a one-temperature model in the RFB, with temperature T_0, the second temperature T being the result of the kinematics in passing from the RFB to the CMS. However, this interpretation, as we shall see, contradicts other characteristics of the model. Moreover, at present we cannot say whether the model can be interpreted in terms of fireballs and, if so, how many and with what distribution of velocities.

The difficulty appears when we try to reconcile the fireball origin of the model with the resulting angular distribution.

D. Angular Distribution in Log Tan $(\theta*/2)$

In cosmic-ray jets, the angular distribution of secondary particles in the variable $x = \log \tan (\theta*/2)$, where $\theta*$ is the angle of a particle with respect to the forward-backward direction, has frequently two peaks (this feature gave origin to the two-fireballs model).

We shall obtain and analyze the log tan $(\theta*/2)$ distribution one obtains from the two-temperature model.

In general, if x_1 and x_2 are two independent random variables with probability distributions $f_1(x_1)$ and $f_2(x_2)$, then the new random variable $y = \varphi(x_1, x_2)$ has the probability distribution

$$f(y) = \int_{x_1} dx_1\, f_1(x_1)f_2(x_2) \Big/ \frac{\partial \varphi}{\partial x_2}, \tag{54}$$

where the integrand must be expressed in terms of x_1 before the integration is performed. If the criterion given by Eq. 54 is applied to the transformation

$$y_1 = \tan \theta* = p_t^*/p_\ell^*,$$

and further the following changes of variable are made:

$$y_2 = \tan (\theta*/2), \text{ given in implicit form by } y_1 = \frac{2y_2}{1 - y_2^2},$$

and

$$x = \log y_2 = \frac{1}{2.3} \ln y_2,$$

then, using the distributions given in Eq. 53, we obtain the angular-distribution function in the form

$$F(x) = \frac{2.3\ T}{m^4 c^5 T_0 K_2(mc^2/T_0) K_2(mc^2/T)} \frac{\cosh 2.3\ x}{\sinh^3 |2.3\ x|}$$

$$\times \int_0^\infty p_\ell^{*2} \left(\frac{p_\ell^{*2}}{\sinh^2 2.3\ x} + m^2\right)^{1/2} K_1\left[\frac{1}{T_0}\left(\frac{p_\ell^{*2}}{\sinh^2 2.3\ x} + m^2\right)^{1/2}\right]$$

$$\times \exp(-\mu_1^*/T)(1 + \mu_1^*/T)\ dp_\ell^* . \tag{55}$$

This function is represented in Fig. 9 as T_0 increases and in Fig. 10 as T decreases toward T_0. It can be observed that the two-peaked feature is strongly related to the model and is controlled by these two variables. The case of decreasing T corresponds to decreasing length of the longitudinal half-axis of the ellipsoid of constant momentum in the CMS, and hence this actually becomes the RFB (where we have a sphere of constant momentum). This can be more easily visualized by considering Fig. 11. The case of increasing T_0, even if it does not really occur, because T_0 has an upper limit (say 0.16 GeV), represents an increasing transversal half-axis of the

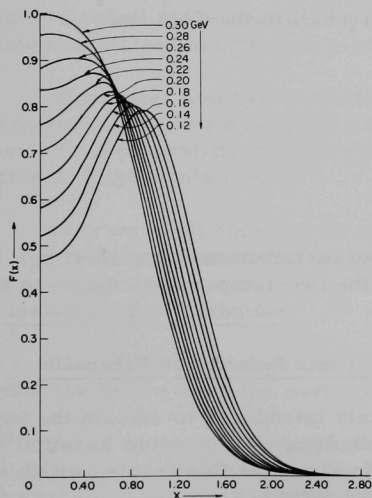
Fig. 9. Angular Distribution Function F(x), for x > 0 for Different Values of T_0 at E_0 = 3000 GeV and m = 0.141 GeV/c^2. ANL Neg. No. 145-1207 Rev. 1.
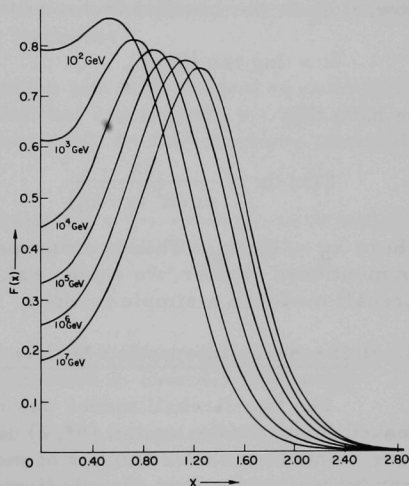
Fig. 10. Angular Distribution Function F(x), for x > 0 for Different Values of E_0 (primary energy) at T_0 = 0.14 GeV and m = 0.141 GeV/c^2. ANL Neg. No. 145-1208 Rev. 1.
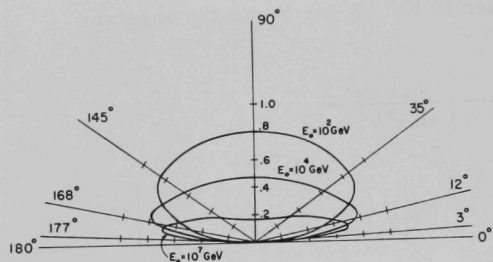
Fig. 11. Polar Representation of the Angular Distribution Function in Terms of the Angle θ^* in the CMS, for Different Values of E_0 (primary energy). ANL Neg. No. 145-1209 Rev. 1.

ellipsoid of constant momentum in the CMS. This could lead one to think that the longitudinal temperature is a kinematic effect which results when we go from the RFB to the CMS.[38]

However, we can show that if we consider a one-fireball model with a temperature T_0 in the RFB, we always obtain a one-peaked log tan $(\theta^*/2)$ distribution in the CMS. In fact, the angular distribution in the RFB is

$$\frac{d\Omega}{4\pi},$$

where $d\Omega$ is a differential solid angle whose axis forms an angle θ with the forward-backward direction. This means a distribution of the form

$$\sin \theta \, d\theta.$$

Now, if γ_b is the Lorentz factor of the fireball in the CMS and

$$x = \log \tan (\theta^*/2),$$

we have that

$$F(x) \, dx = \frac{dx}{\cosh^2 (x + x_b)}, \qquad (56)$$

where $x_b = \log \gamma_b$. This is a one-peaked distribution centered at x_b. Thus, as mentioned earlier, we cannot relate the two-temperature model to a one-fireball model in a simple manner.

E. High-energy Interaction Models and Their Relation to Fireballs

The two-fireball model was mainly introduced to explain the two-peaked feature of the log tan $(\theta^*/2)$ distribution. Daiborg and Rozental[39] have pointed out that a number of models also give this feature with a transversal momentum distribution of the form

$$W_\perp(p_\perp^*) \, dp_\perp^* = \text{const} \, p_\perp^* \exp(-p_\perp^*/p_0) \, dp_\perp^*.$$

They affirm that the two peaks are a consequence of increasing the ratio $p_\ell/p_\perp$ as E_0 increases. This could be interpreted to mean that a two-fireball model is unnecessary. However, the same calculations carried

out[40] with a transversal distribution of the form

$$W_\perp(p_\perp^*) \, dp_\perp^* = \text{const } p^{*3/2} \exp(-p_\perp^*/p_0)$$

raise doubt on the conclusions obtained by Daiborg and Rozental.

On the other hand, we have just seen that the two-temperature model also gives two peaks.

The fact that all these models predict two-peaked angular distribution does not exclude the existence of two fireballs. In fact the two-temperature model in particular, could be related to an unknown number of fireballs where we have an unknown velocity distribution in the CMS.

With Eq. 56 for one fireball moving in the CMS with a Lorentz factor γ_b, we could obtain the log tan $(\theta^*/2)$ distribution for an infinite number of fireballs with a distribution $\varphi(\gamma_b) \, d\gamma_b$ for their Lorentz factor in the form

$$F(x) \, dx = dx \int_{\gamma_b} \frac{\varphi(\gamma_b)}{\cosh^2 (x + x_b)} \, d\gamma_b. \qquad (57)$$

If we use for $\varphi(\gamma_b)$ the distribution obtained by Hagedorn for his continuum infinite-fireball model we find[41] a one-peaked distribution for both "newly created particles" and "through-going particles."

Since one- and two-peaked features are both present in cosmic-ray interactions, we should look for a model that can account for this joint behavior. A possibility of achieving this could be that of adding convective motion to Hagedorn's model.[41]

Now we shall concentrate on obtaining some predictions on inelasticity and multiplicity distributions from the two-temperature model.

F. Inelasticity Distribution

One of the main tasks of any model of high-energy interactions is to predict the behavior of the particle production at cosmic-ray energy.

After having interpreted the two-temperature model, we shall compare it with other models, say the two-fireball and the CKP models, at such high energies. One way of doing it is to obtain the inelasticity distribution as predicted by each model.

For simplicity, the pion inelasticity distribution in the CMS, $W(K_\pi^*)$, will be obtained. Given the longitudinal and transverse momentum distributions in the CMS, say $f(p_\ell^*) \, dp_\ell^*$ and $g(p_t^*) \, dp_t^*$, and the mean multiplicity

n_π corresponding to the energy under consideration, 1000 jets are generated and the frequency distribution for the pion inelasticity is calculated as follows:

1. Obtain $F(p_\ell^*) = \int_0^{p_\ell^*} f(x)\, dx$, $G(p_t^*) = \int_0^{p_t^*} g(x)\, dx$, and their inverse F^{-1} and G^{-1}.

2. Generate n_π uniformly distributed random numbers $\xi_1,\ \xi_2,\ \ldots,\ \xi_n$, where n_π is even.

3. Calculate $n_\pi/2$ f-distributed random numbers $p_{\ell_i}^* = F^{-1}(\xi_i)$, $i = 1,\ \ldots,\ n_\pi/2$, and $n_\pi/2$ g-distributed random numbers $p_{t_i}^* = G^{-1}(\xi_i)$, $i = n_\pi/2 + 1,\ \ldots,\ n_\pi$.

4. Calculate the amount of CMS energy that goes into pions, E_π^*.

5. Calculate the value of the inelasticity, and repeat the procedure.
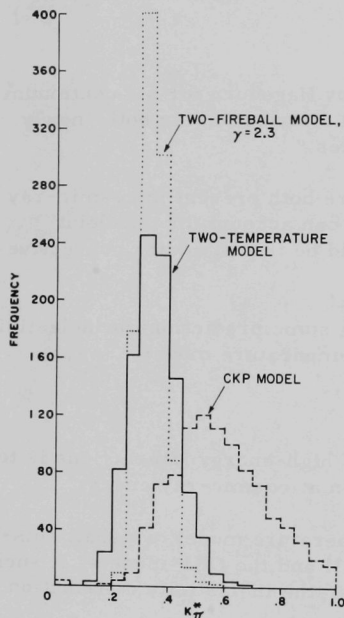
Fig. 12

Pion Inelasticity Distribution in the CMS for Different Models at a Primary Energy of 3000 GeV. ANL Neg. No. 145-1206 Rev. 1.

The energy-momentum conservation requirements are automatically satisfied, since we are sampling from the distributions $f(p_\ell^*)$ and $g(p_t^*)$. In fact, in the actual calculations, only about 0.5% of the jets had to be rejected. For the two-fireball model, E_π is calculated in the RFB with an isotropic particle distribution, i.e., $f(p_\ell^*) \equiv g(p_t^*)$, and then E_π^* in the CMS is obtained by multiplying by the Lorentz factor γ for going from RFB to the CMS. Since the two-fireball model does not give any momentum distribution, the choice $g(p_t^*) = W_t^*(p_t^*)$ given by Eq. 51 was taken and γ was selected in such a way that the mean values of K_π^* given by the two-temperature and the two-fireball models were the same. The resulting distributions are shown in Fig. 12. They are very different for the two-temperature and the CKP models. The mean value predicted by CKP is about 0.57, and that predicted by the two-temperature model is about 0.37. Experimental observations[35] seem to favor the last one.

Figure 13 shows the inelasticity distribution for the two-temperature model at different values of the primary energy.
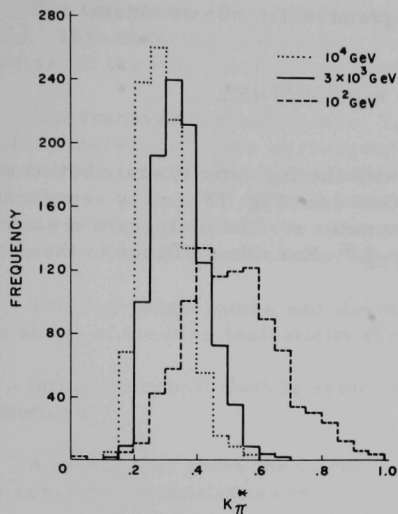
Fig. 13

Pion Inelasticity Distribution in the CMS for the Two-temperature Model at Different Values of Primary Energy. ANL Neg. No. 145-1266 Rev. 1.

G. Multiplicity Distribution

Let $q(n|E_\pi^*)\, dE_\pi^*$ be the conditional probability of producing $\bar{n}$ pions (π^+, π^-, π^0), given that a CMS energy $E_\pi^* \in (E_\pi^*, E_\pi^* + dE_\pi^*)$ is left to the pion component. That is to say, if E_0^* is the total energy available in the CMS and K_π^* is the inelasticity, then

$$E_\pi^* = K_\pi^* E_0^*.$$

If $W(K_\pi^*)\, dK_\pi^*$ is the probability that an event occurs with inelasticity $K_\pi^* \in (K_\pi^*, K_\pi^* + dK_\pi^*)$, then the multiplicity distribution is given by

$$p(n) = \frac{1}{E_0^*} \int_0^{E_0^*} W(E_\pi^*/E_0^*) q(n|E_\pi^*)\, dE_\pi^*. \tag{58}$$

Now, suppose that the chance for a particle to be "boiled off" decreases exponentially with the energy E_π^* left to the pion component (not with the total energy E_0^*).

This implies that $q(n|E_\pi^*)$ is given by a Poisson distribution,

$$q(n|E_\pi^*)\, dE_\pi^* = \frac{(\alpha E_\pi^*)^n}{n!} \exp(-\alpha E_\pi^*)\, dE_\pi^*, \tag{59}$$

where the mean number α of particles (pions) produced per unit energy will depend on the total energy E_0^*. However, we do not know this dependence and, rather, will use α as a parameter to fit the experimental data.

Introducing Eq. 59 in the integrand of Eq. 58, we obtain

$$p(n) = \frac{1}{E_0^*} \int_0^{E_0^*} W\left(\frac{E_\pi^*}{E_0^*}\right) \frac{(\alpha E_\pi^*)^n}{n!} \exp(-\alpha E_\pi^*) \, dE_\pi^*. \tag{60}$$

This probability has been computed with the inelasticity distribution obtained with the Monte Carlo method at 100 GeV (see Fig. 13) and is represented in Fig. 14 for several values of the parameter α. The histogram represents the experimental data of Abraham et al.[42] For other fittings to the experimental data, see Imaeda.[43]
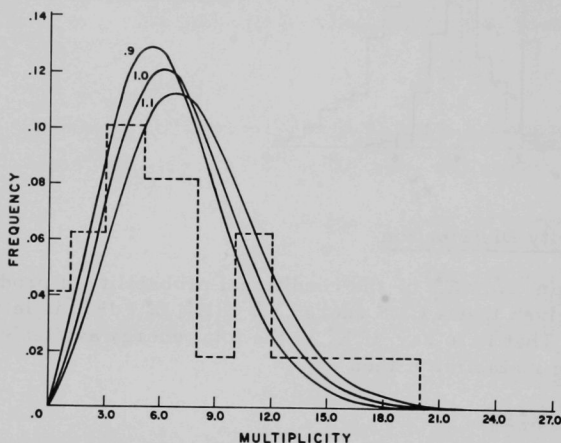
Fig. 14. Pion Multiplicity Distribution at Different Values of the Parameter α, Compared with Experimental Results (histogram). ANL Neg. No. 145-1268.

We have not been able to prove the assumption (Eq. 59), but there are other indications that it may not be too far from reality.[44] We feel that the answer may be in constructing a stochastic process model for the conditional probability $q(n|E_\pi^*)$ based on the ideas of the statistical thermodynamic approach.

H. Conclusions

Several semiempirical models of high-energy interactions predict a double-peaked angular distribution in $\log \tan (\theta^*/2)$ of the produced particles. This feature is most pronounced in the two-temperature model. Up to the present, a relation has not been found between them and the fireballs; however, the two-peaked feature is not an exclusive characteristic of the two-fireball model.

The two peaks disappear as the incident energy is decreased (i.e., $T \rightarrow T_0$). This observed feature has a completely natural explanation in the context of the two-temperature model.

The transverse temperature, T_0, decreases as the mass of the secondary increases. This corresponds to a decrease in the thermal motion of the particles being "boiled off." Then, as T_0 grows, the angular distribution in log tan $(\theta^*/2)$ will become more and more flat, turning toward a single peak. However, this situation will not be reached because, since the lowest mass particles produced are pions, T_0 has an upper bound.

The two-temperature and the two-fireball models agree quite well on the shape of the pion inelasticity distribution at cosmic-ray energies.

Infinite-fireball models seem to lead to single-peaked log tan $(\theta^*/2)$ distributions.

A model that gives the correct single or double peaked behavior in the correct circumstances is still unknown.

V. THE NUCLEAR ACTIVE COMPONENT OF EXTENSIVE AIR SHOWERS

A. Introduction

In contrast with the three-dimensional electron-photon cascade problem whose solution has been extensively discussed, the three-dimensional nucleon-pion cascade equations have not been solved analytically, due to the complexity of the production cross sections. However, some Monte Carlo calculations have been made.[45,46]

A new concept on the particle generation, based on the number of pion links found in tracing a particle back to the primary cosmic ray, introduced by Narayan and Yodh[47] and later modified by Dedenko,[48] has been successful as a fast semianalytical method to solve the nucleon-pion equations in one dimension.

In this chapter the "pion links method" will be developed in order to obtain the lateral and angular structure functions of the nuclear active component of cosmic-ray showers. Computed results will be presented for the lateral structure function for showers produced in the atmosphere and in the ionization calorimeter.

Several groups[49-51] are engaged in measuring the total nuclear cross sections at cosmic-ray energies due to the importance that the behavior of this quantity at very high energy has in establishing the validity of different

elementary particle models. Solutions for the lateral structure function of the nuclear active component of cosmic rays, as accurate as possible, are of great importance to those experiments.

B. Mathematical Formulation

Let $N(E, \underline{r}, \underline{\theta}, t)\, dEd\underline{r}d\underline{\theta}$ and $\Pi(E, \underline{r}, \underline{\theta}, t)\, dEd\underline{r}d\underline{\theta}$ be the number of nucleons and pions, respectively, in the energy interval $(E, E + dE)$, in the radial vector interval $(\underline{r}, \underline{r} + d\underline{r})$ and in the angle interval $(\underline{\theta}, \underline{\theta} + d\underline{\theta})$, at a depth t, produced by a primary of energy E_0. The variables $\underline{r}$ and $\underline{\theta}$ are illustrated in Fig. 15. The quantities of interest are the radial and angular structure functions given by

$$N_1(E, r, t) = \iint\limits_{-\infty}^{\infty} N(E, \underline{r}, \underline{\theta}, t)\, d\underline{\theta}$$

and

$$N_2(E, \theta, t) = \iint\limits_{-\infty}^{\infty} N(E, \underline{r}, \underline{\theta}, t)\, d\underline{r}$$

for the nucleons, and the same for the pions, say $\Pi_1(E, r, t)$ and $\Pi_2(E, r, t)$. The production cross sections for each individual high-energy collision are given by $S_{AB}(E, E', \underline{\theta} - \underline{\theta}')\, dEd\underline{\theta}$, which represent the number of particles of type A in the energy interval $(E, E + dE)$ and in the angle interval $(\underline{\theta}, \underline{\theta} + d\underline{\theta})$ produced by a particle of type B, energy E', and direction of motion $\underline{\theta}'$, given that a collision occurred with a nucleus of the absorber.

We will assume that S_{NN} and $S_{N\pi}$ are homogeneous functions of the energy variables, that is to say, they are of the form $(1/E')S_{NN}(E/E', \underline{\theta} - \underline{\theta}')$ and $(1/E')S_{N\pi}(E/E', \underline{\theta} - \underline{\theta}')$, respectively. There will be no such restriction on $S_{\pi N}$ and $S_{\pi\pi}$.
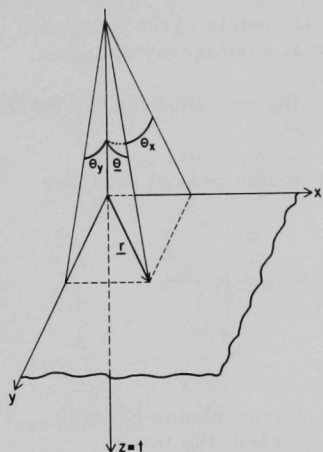
Fig. 15

Spatial and Angular Coordinates for the Three-dimensional Cascade. ANL Neg. No. 145-1250.

If t is measured in units of the nucleon-interaction mean free path λ_N, $N(E, \underline{r}, \underline{\theta}, t)$ and $\Pi(E, \underline{r}, \underline{\theta}, t)$ satisfy the following system of integro-differential equations:

$$\left(\frac{\partial}{\partial t} + \underline{\theta} \cdot \frac{\partial}{\partial \underline{r}}\right) N(E, \underline{r}, \underline{\theta}, t) = -N(E, \underline{r}, \underline{\theta}, t)$$

$$+ \int_E^{\infty} dE' \iint\limits_{-\infty}^{\infty} d\underline{\theta}' \left[(1/E')S_{NN}(E/E', \underline{\theta} - \underline{\theta}')\, N(E', \underline{r}, \underline{\theta}', t) \right.$$

$$\left. + \frac{\lambda_N}{\lambda_\pi} \frac{1}{E'} S_{N\pi}(E/E', \underline{\theta} - \underline{\theta}')\, \Pi(E', \underline{r}, \underline{\theta}', t) \right]$$

(61)
(Contd.)

and

$$\left(\frac{\partial}{\partial t} + \underline{\theta} \cdot \frac{\partial}{\partial \underline{r}}\right) \Pi(E, \underline{r}, \underline{\theta}, t) = -\left(\frac{\lambda_N}{\lambda_\pi} + \frac{\beta}{Et}\right) \Pi(E, \underline{r}, \underline{\theta}, t)$$

$$(61)$$

$$+ \int_E^\infty dE' \iint_{-\infty}^\infty d\underline{\theta}' \left[S_{\pi N}(E, E', \underline{\theta} - \underline{\theta}') \, N(E', \underline{r}, \underline{\theta}', t) \right.$$

$$\left. + \frac{\lambda_N}{\lambda_\pi} S_{\pi\pi}(E, E', \underline{\theta} - \underline{\theta}') \, \Pi(E', \underline{r}, \underline{\theta}', t) \right],$$

where β is the decay parameter of the charged pions.

If we introduce the double Fourier transform

$$\hat{f}(E, \underline{\rho}, \underline{\Lambda}, t) = \frac{1}{4\pi^2} \iiint_{-\infty}^\infty \exp[i(\underline{r} \cdot \underline{\rho} + \underline{\theta} \cdot \underline{\Lambda})] \, f(E, \underline{r}, \underline{\theta}, t) \, d\underline{r} d\underline{\theta}, \qquad (62)$$

the nucleon lateral structure function will be given by

$$N_1(E, r, t) = \iint_{-\infty}^\infty N(E, \underline{r}, \underline{\theta}, t) \, d\underline{\theta}$$

$$= \iint_{-\infty}^\infty e^{-i\underline{r} \cdot \underline{\rho}} \, \hat{N}(E, \underline{\rho}, 0, t) \, d\underline{\rho} \qquad (63)$$

$$= \int_0^\infty 2\pi\rho \hat{N}(E, \rho, 0, t) J_0(r\rho) \, d\rho,$$

where the relation

$$J_0(r\rho) = \frac{1}{2\pi} \int_0^{2\pi} e^{-ir\rho \cos\varphi} \, d\varphi$$

has been used.

By the same arugment,

$$N_2(E, \theta, t) = \int_0^\infty 2\pi\Lambda \hat{N}(E, 0, \Lambda, t) J_0(\theta\Lambda) \, d\Lambda, \qquad (64)$$

and the same is applicable to $\Pi_1(E, r, t)$ and $\Pi_2(E, \theta, t)$.

If the operators Γ_{AB} are defined by

$$\Gamma_{AB}\hat{B}(E, \underline{\rho}, \underline{\Lambda}, t) = \int_E^\infty dE' \, \hat{S}_{AB}(E, E', \underline{\Lambda})\hat{B}(E', \underline{\rho}, \underline{\Lambda}, t) \qquad (65)$$

the system of Eqs. 61 is transformed by the double Fourier transform (Eq. 62) into

$$\left(\frac{\partial}{\partial t} - \underline{\rho} \cdot \frac{\partial}{\partial \underline{\Lambda}} + 1 - \Gamma_{NN}\right) \hat{N}(E, \underline{\rho}, \underline{\Lambda}, t) = \frac{\lambda_N}{\lambda_\pi} \Gamma_{N\pi}\hat{\bar{\Pi}}(E, \underline{\rho}, \underline{\Lambda}, t);$$

$$\left(\frac{\partial}{\partial t} - \underline{\rho} \cdot \frac{\partial}{\partial \underline{\Lambda}} + \frac{\lambda_N}{\lambda_\pi} + \frac{\beta}{Et} - \frac{\lambda_N}{\lambda_\pi} \Gamma_{\pi\pi}\right) \hat{\bar{\Pi}}(E, \underline{\rho}, \underline{\Lambda}, t) = \Gamma_{\pi N}\hat{N}(E, \underline{\rho}, \underline{\Lambda}, t). \qquad (66)$$

To obtain the lateral structure functions, we must take the solution of Eqs. 66 at $\underline{\Lambda} = 0$. To achieve this, the vector $\underline{\Lambda}$ is first decomposed in two components, one parallel and one perpendicular to $\underline{\rho}$, say Λ_1 and Λ_2. Then Λ_2 is put equal to zero in the resulting equations, and finally the following change of variables is made:

$$t' = t, \quad \rho' = \rho, \quad \gamma = \frac{\Lambda_1}{\rho} + t.$$

The resulting system of equations is

$$\left.\begin{aligned}\left(\frac{\partial}{\partial t} + 1 - \Gamma_{NN}\right) \hat{N}(E, \rho, \rho(\gamma - t), t) &= \frac{\lambda_N}{\lambda_\pi} \Gamma_{N\pi}\hat{\bar{\Pi}}(E, \rho, \rho(\gamma - t), t); \\ \left(\frac{\partial}{\partial t} + \frac{\lambda_N}{\lambda_\pi} + \frac{\beta}{Et} - \frac{\lambda_N}{\lambda_\pi} \Gamma_{\pi\pi}\right) \hat{\bar{\Pi}}(E, \rho, \rho(\gamma - t), t) &= \Gamma_{\pi N}\hat{N}(E, \rho, \rho(\gamma - t), t).\end{aligned}\right\} \qquad (67)$$

The solutions of the system of Eqs. 67, taken at $\gamma = t$, will yield $\hat{N}_1(E, \rho, t)$ and $\hat{\bar{\Pi}}_1(E, \rho, t)$ which, by Eq. 63, are the Hankel transforms of the nucleon and pion structure functions, respectively.

The Hankel transforms for the angular structure functions can be obtained directly by making $\underline{\rho} = 0$ in Eq. 66.

The numerical solutions of the system (Eqs. 67) at $\gamma = t$ will be a pair of three-dimensional matrices whose elements are given by

$$\hat{N}_1(E_i, \rho_j, t_k) \text{ and } \hat{\bar{\Pi}}_1(E_i, \rho_j, t_k).$$

Using the method of the pion links, to be discussed in Section C below, we can obtain these matrices by slices determined by energy intervals.

C. The Pion-link Method

One characteristic of the high-energy interactions is that only a small number of nucleons is produced, and they carry away a considerable amount of energy, while a large number of pions share the rest of the energy. No forward pion has been observed carrying a predominant amount of the available energy. This fact suggests the following way of defining the particle generation in the nuclear active component of a cosmic-ray shower: A particle (nucleon or pion) will be regarded as belonging to the nth generation if, when traced back to the primary cosmic ray, exactly n pion links are found.

Let $E_{0,max}^{\pi}$ be the maximum energy observed among pions of the zeroth generation, $E_{1,max}^{\pi}$ the maximum for the first generation, and so on. Analogously, let $E_{0,max}^{N}$, $E_{1,max}^{N}$, ..., be the maximum energies for the different generations of nucleons. Then, if

$$\Delta E_i^{\pi} = E_{i-1,max}^{\pi} - E_{i,max}^{\pi}$$

and

$$\Delta E_i^{N} = E_{i-1,max}^{N} - E_{i,max}^{N},$$

in the slices determined by the energy intervals ΔE_i^{N} and ΔE_i^{π} Eqs. 67 become

$$\left(\frac{\partial}{\partial t} + 1 - \Gamma_{NN}\right) \hat{N}_1^{(1)}(E, \rho, t) = 0$$

and

$$\left(\frac{\partial}{\partial t} + \frac{\lambda_N}{\lambda_\pi} + \frac{\beta}{Et}\right) \hat{\Pi}_1^{(1)}(E, \rho, t) = \Gamma_{\pi N} \hat{N}_1^{(1)}(E, \rho, t), \tag{68}$$

and, in general, for the nth slice with $n \geq 2$,

$$\left(\frac{\partial}{\partial t} + 1 - \Gamma_{NN}\right) \hat{N}_1^{(n)}(E, \rho, t) = \frac{\lambda_N}{\lambda_\pi} \Gamma_{N\pi} \hat{\Pi}_1^{(n-1)}(E, \rho, t)$$

and

$$\left(\frac{\partial}{\partial t} + \frac{\lambda_N}{\lambda_\pi} + \frac{\beta}{Et}\right) \hat{\Pi}_1^{(n)}(E, \rho, t) = \Gamma_{\pi N} \hat{N}_1^{(n)}(E, \rho, t) + \frac{\lambda_N}{\lambda_\pi} \Gamma_{\pi\pi} \hat{\Pi}_1^{(n-1)}(E, \rho, t). \tag{69}$$

The integration domains of the operators Γ_{AB} must be the same as the energy domains on which each function is defined. The second equations of Eqs. 68 and 69 are simple linear differential equations of the first order, and their solution is

$$\hat{\Pi}_1^{(n)}(E, \rho, t) = \exp\left(-\frac{\lambda_N}{\lambda_\pi} t\right) \int_0^t d\tau \left(\frac{\tau}{t}\right)^{\beta/E} \exp\left(\frac{\lambda_N}{\lambda_\pi} \tau\right) \left[\Gamma_{\pi N} \hat{N}_1^{(n)}(E, \rho, \tau)\right.$$

$$\left. + \frac{\lambda_N}{\lambda_\pi} \Gamma_{\pi\pi} \hat{\Pi}_1^{(n-1)}(E, \rho, \tau)\right]. \tag{70}$$

Then it is clear the Eq. 68 can be solved first for $\hat{N}_1^{(1)}$, and this will determine the function $\hat{\Pi}_1^{(1)}$ which determines $\hat{N}_1^{(2)}$ in Eq. 69, and so on.

It only remains to solve the first of Eqs. 69. This is an integro-differential equation with the general "source term"

$$\hat{f}_1^{(n-1)}(E, \rho, t) = \frac{\lambda_N}{\lambda_\pi} \Gamma_{N\pi} \hat{\Pi}_1^{(n-1)}(E, \rho, t)$$

$$= \frac{\lambda_N}{\lambda_\pi} \int_E^\infty \frac{dE}{E'} \hat{S}_{N\pi}(E/E', \rho, t)\hat{\Pi}_1^{(n-1)}(E', \rho, t),$$

which is different for different slices. Because of the assumed form of S_{NN} and $S_{N\pi}$, the first of Eqs. 69 can be solved by using the Mellin transform defined by

$$\hat{g}(s) = \int_0^\infty x^s g(x)\, dx, \quad g(x) = \frac{1}{2\pi i} \int_{\delta-i\infty}^{\delta+i\infty} \frac{\hat{g}(s)}{x^{s+1}}\, ds.$$

Using the initial condition

$$N_1(E, r, t)\big|_{t=0} = \delta(E - E_0) \frac{\delta(r)}{2\pi r},$$

we obtain the solution

$$\hat{N}_1^{(n)}(E, \rho, t) = \frac{1}{2\pi i} \int_{\delta-i\infty}^{\delta+i\infty} \frac{1}{E^{s+1}} \exp\left[\int_0^1 \int_0^t \hat{S}_{NN}(q, \rho, t')q^s\, dqdt' - t\right]$$

$$\times\, [E_0^s + F_1^{(n-1)}(s, \rho, t)]\, ds, \tag{71}$$

where

$$F_1^{(n-1)}(s, \rho, t) = \int_0^t d\tau\, \hat{f}_1^{(n-1)}(s, \rho, \tau) \exp\left\{-\left[\int_0^1 \int_0^\tau \hat{S}_{NN}(q, \rho, \tau')q^s\, dqd\tau' - \tau\right]\right\}. \tag{72}$$

For the Hankel transform of the integral lateral structure function given by

$$\hat{N}_1^{(n)}(>E, \rho, t) = \int_E^{\infty} \hat{N}_1^{(n)}(E', \rho, t)\, dE'$$

$$= \frac{1}{2\pi i} \int_{\delta-i\infty}^{\delta+i\infty} \frac{ds}{s} E^{-s} \exp\left[\int_0^1 \int_0^t \hat{S}_{NN}(q, \rho, t')q^s\, dq dt' - t\right]$$

$$\times [E_0^s + F_1^{(n-1)}(s, \rho, t)], \tag{73}$$

the integration can be carried out by the saddle-point method and the result is given in the parametric form

$$\hat{N}_1^{(n)}(>E, \rho, t) = \frac{\exp\left[\int_0^1 \int_0^t \hat{S}_{NN}(q, \rho, t')q^s\, dq dt' - t\right]\left[E_0^s + F_1^{(n-1)}(s, \rho, t)\right]}{sE^s \sqrt{2\pi\left(\frac{\partial^2}{\partial s^2}\left\{\int_0^1 \int_0^t \hat{S}_{NN}(q, \rho, t')q^s\, dq dt' + \ln\left[E_0^s + F_1^{(n-1)}(s, \rho, t)\right]\right\} + \frac{1}{s^2}\right)}}. \tag{74}$$

$$\frac{\partial}{\partial s} \int_0^1 \int_0^t \hat{S}_{NN}(q, \rho, t')q^s\, dq dt' + \left[E_0^s + F_1^{(n-1)}(s, \rho, t)\right]^{-1}\left[E_0^s \ln E_0 + \frac{\partial}{\partial s} F_1^{(n-1)}(s, \rho, t)\right] - \ln E = \frac{1}{s}. \tag{75}$$

D. Particles Production Cross Sections and Results

In the present calculations, the following production cross sections were chosen:[52]

$$S_{NN}(E, E_0, \theta) = n\delta\left(E - \frac{\gamma}{n} E_0\right) \frac{\delta(\theta)}{2\pi\theta}, \tag{76}$$

$$S_{N\pi}(E, E_0, \theta) = \delta(E - \eta E_0) \frac{\delta(\theta)}{2\pi\theta}, \tag{77}$$

and

$$S_{\pi N}(E, E_0, \theta) = \frac{n_\pi E^2}{2\pi p_0^2 c^2 T} \exp\left[-E\left(\frac{1}{T} + \frac{\theta}{p_0 c}\right)\right], \tag{78}$$

where

$$n_\pi = \alpha E_0^{1/4}$$

is the mean pion multiplicity, and

$$T = \frac{K_\pi}{\alpha} E_0^{3/4}$$

is the mean energy carried out by a single pion.

The expression for $S_{\pi\pi}(E, E_0, \theta)$ is the same as Eq. 78 with different value of the inelasticity K_π. The values chosen for the parameters are given in Table III.

TABLE III. Parameters for Production Cross Sections

n	γ	η	$p_0 c$	K_π (nucleon)	K_π (pion)	α
2	0.5	0.002	0.18 GeV	0.5	1.0	2.7

Using these production cross sections the functions $\hat{S}_{\pi N}[E, E', \rho(\gamma - t)]$ and $\hat{S}_{\pi\pi}[E, E', \rho(\gamma - t)]$ in the integrand of Eq. 5 take the form

$$\frac{\alpha^2}{2\pi p_0^2 c^2 K_\pi} E'^{-1/2} \exp[-(\alpha/K_\pi)(E/E')^{3/4}] \left\{ 1 + \left[p_0 c - \frac{\rho(\gamma - t)}{E} \right]^2 \right\}^{-3/2}. \tag{79}$$

This will be responsible for the radial dependence of the lateral structure function. Because the factor α/K_π is smaller for pion-nucleon scattering than for nucleon-nucleon scattering, the term $\Gamma_{\pi\pi} \hat{\Pi}_1^{(n)}(E, \rho, t)$ is the one that grows faster, so even a low-energy nucleon can produce a considerable number of particles.

Since the main difference among several multiple particle production models is in the transversal momentum distribution, Eq. 79 will be different for each model and will probably cause appreciable differences in the lateral structure function, providing thus a way to test those models.

A FORTRAN IV program, discussed in the appendix, has been written following the scheme of Section C above. The different slices were taken such that $\Delta E_1 = E_0 - E_{\pi,1}$, $\Delta E_2 = E_{\pi,1} - E_{\pi,2}$, etc., where

$$E_{\pi,1} = (K_\pi/\alpha)E_0^{3/4}, \quad E_{\pi,2} = (K_\pi/\alpha)E_{\pi,1}^{3/4},$$

and so on, but the results are not very sensitive to the choice of the energy intervals. In each slice, the "age" parameter s is computed as a function of E, ρ, and t by finding the roots of Eq. 75. However, the contribution from $\Gamma_{N\pi} \hat{\Pi}_1^{(n)}(E, \rho, t)$ is negligible at energies lower than about 10^5 GeV.[47] In that case, $\hat{N}_1^{(n)}$ is independent of ρ, and by Eq. 63,

$$N_1(E, r, t) = N_1(E, t) \frac{\delta(r)}{2\pi r}.$$

Results were obtained for primary nucleons of 10^4, 10^5, and 10^6 GeV for showers developing in the atmosphere, as well as in an ionization calorimeter. They are represented in Figs. 16-22. All figures refer to the number of particles with energy $E > 2$ GeV.

Fig. 16. Integral Lateral Structure Function for the Atmosphere at $E_0 = 10^6$ GeV. ANL Neg. No. 145-1252 Rev. 1.
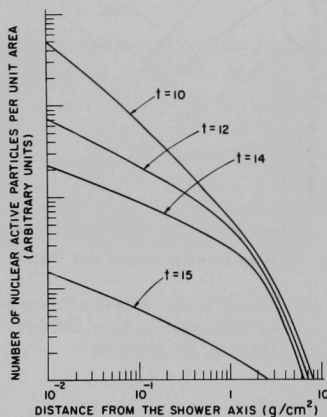
Fig. 17. Integral Lateral Structure Function for the Ionization Calorimeter at $E_0 = 10^6$ GeV. ANL Neg. No. 145-1249.
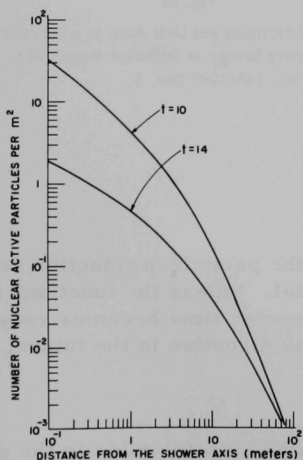
Fig. 18. Integral Lateral Structure Function for the Atmosphere at $E_0 = 10^5$ GeV. ANL Neg. No. 145-1251.

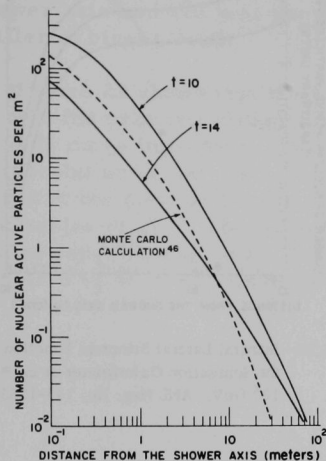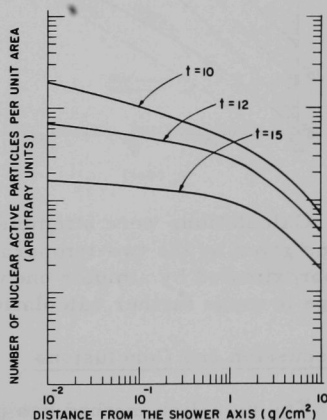Fig. 19. Integral Lateral Structure Function for the Ionization Calorimeter at $E_0 = 10^5$ GeV. ANL Neg. No. 145-1259.
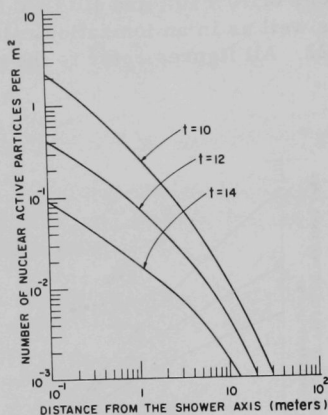
Fig. 20. Integral Lateral Structure Function for the Atmosphere at $E_0 = 10^4$ GeV. ANL Neg. No. 145-1248.
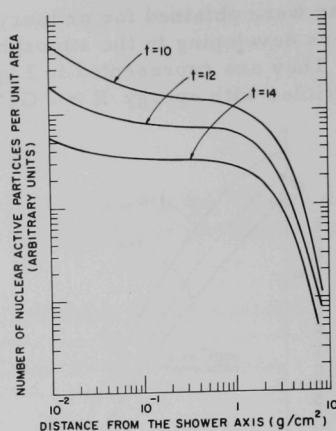
Fig. 21. Integral Lateral Structure Function for the Ionization Calorimeter at $E_0 = 10^4$ GeV. ANL Neg. No. 145-1253.
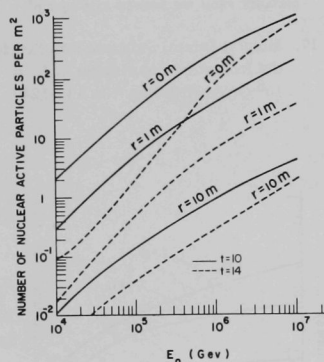
Fig. 22

Number of Particles per Unit Area as a Function of the Primary Energy at Different Values of r. ANL Neg. No. 145-1247 Rev. 1.

Calculations were attempted using the particle-production cross sections given by the two-temperature model. Unless the functions involved are approximated by simpler ones, the computer time becomes very large. We hope to make further calculations in this direction in the future.

E. Discussion and Conclusions

The pion-link method has proved to be a useful guide in the physical interpretation of the development of the nuclear active component of one-dimensional extensive air showers.[47] It gives a most important role to pion-nucleon collisions.

Comparing the lateral structure function for the same primary energy in the atmosphere and in the ionization calorimeter, we see that in the last case the curves are more flat. This is a consequence of the fact that the decay affects more those pions that are farther away from the shower axis and are less energetic. As could be expected, the effect is smaller at bigger depth.

Figure 22 shows that the number of particles per unit area grows faster with the primary energy for small values of r, where the $S_{\pi\pi}$ contribution is more important. Figure 16 compares this with the Monte Carlo calculation of Ref. 46. The Monte Carlo curve drops out too fast compared to the measurements of Abrosimov et al.,[53] Nikolsky et al.,[54] and Chatterjee et al.[55] The curves calculated here are in good agreement with those experimental data. Finally, the method used here has proven to be fast: For $E_0 = 10^6$ GeV, the computing time is less than 30 min.

APPENDIX

A FORTRAN IV Program to Compute the Lateral Structure Function
of the N-component of Extensive Air Showers

1. Definition of the Most Relevant Quantities Involved in the Program

E0 = Energy of the primary particle (E_0)

BETA = β = decay parameter of pions

PT(I, J, K) = $\hat{N}(E_i, \eta_j, t_k)$

PIT(I, J, K) = $\hat{\Pi}(E_i, \eta_j, t_k)$

PTINT(I, J, K) = $\displaystyle\int_{E_i}^{E_0} \hat{N}(E, \eta_j, t_k)\, dE$

PITINT(I, J, K) = $\displaystyle\int_{E_i}^{E_0} \hat{\Pi}(E, \eta_j, t_k)\, dE$

H1 = $E_i - E_{i+1}$ (different for each slice)

RO = $\rho = e^{-\eta/10^3}$

H2 = $\rho_j - \rho_{j+1}$

H3 = $t_{k+1} - t_k$

S(E, ETA, T) = roots of Eq. 75

$$\text{PINT} = \int_0^t d\tau \left(\frac{\tau}{t}\right)^{\beta/E} \exp\left(\frac{\lambda_N}{\lambda_\pi}\,\tau\right) \left\{ \Gamma_{\pi N}\,\hat{N}_1^{(n)}(E, \eta, \tau) + \frac{\lambda_N}{\lambda_\pi}\,\Gamma_{\pi\pi}\,\hat{\Pi}_1^{(n-1)}(E, \eta, \tau) \right\}$$

of Eq. 70

$$\text{SNNT(S, RO, T)} = \int_0^1 \hat{S}_{NN}(q, \eta, t)\, q^s\, dq$$

$$\text{SNNT1(S, RO, T)} = \frac{\partial}{\partial s}\,\text{SNNT(S, RO, T)}$$

$$\text{SNNT2(S, RO, T)} = \frac{\partial^2}{\partial S^2}\,\text{SNNT(S, RO, T)}$$

$$\text{SNPIT(S, RO, T)} = \int_0^1 \hat{S}_{N\pi}(q, \eta, t)\, q^s\, dq$$

$$\text{SNPIT1}(S, RO, T) = \frac{\partial}{\partial s} \text{SNPIT}(S, RO, T)$$

$$\text{SNPIT2}(S, RO, T) = \frac{\partial^2}{\partial s^2} \text{SNPIT}(S, RO, T)$$

$$\text{SPINT}(E, E1, RO, GAMMA, T)$$

$$= \left[\frac{1}{2\pi} \iint\limits_{-\infty}^{\infty} S_{\pi N}(E, E1, \theta) \exp(i\Lambda_1\theta_1) \, d\theta_1 d\theta_2 \right]_{\Lambda_1 = \rho(\gamma - t)}$$

$$\text{SPIPIT}(E, E1, RO, GAMMA, T)$$

$$= \left[\frac{1}{2\pi} \iint\limits_{-\infty}^{\infty} S_{\pi\pi}(E, E1, \theta) \exp(i\Lambda_1\theta_1) \, d\theta_1 d\theta_2 \right]_{\Lambda_1 = \rho(\gamma - t)}$$

$$FT = F_1^{(n-1)}(s, \eta, t) \text{ given by Eq. 72}$$

$$FT1 = \frac{\partial}{\partial s} FT$$

$$FT2 = \frac{\partial^2}{\partial s^2} FT$$

$$PITT = \hat{\hat{\Pi}}(s, \eta, t) = \int_0^\infty E^s \hat{\Pi}(E, \eta, t) \, dE$$

$$PITT1 = \frac{\partial}{\partial s} PITT$$

$$PITT2 = \frac{\partial^2}{\partial s^2} PITT$$

$$YNT = \Gamma_{\pi N} \hat{N}_1^{(n)}(E, \eta, \tau) + \frac{\lambda_N}{\lambda_\pi} \Gamma_{\pi\pi} \hat{\Pi}_1^{(n-1)}(E, \eta, \tau) \text{ of Eq. 70}$$

$$YNT1 = \frac{\lambda_N}{\lambda_\pi} \Gamma_{\pi\pi} \hat{\Pi}_1^{(n-1)}(E, \eta, \tau)$$

$$YNT2 = \Gamma_{\pi N} \hat{N}_1^{(n)}(E, \eta, \tau).$$

N1, N2, and N3 are the first, second, and third dimensions, respectively, for any matrix involved in the program.

2. Description of the Program

We start by reading the data E_0, β, H2, H3, N2, and N3 and initialize the matrices involved.

The variable ITER numbers the different slices of energy. In the first one, FT, FT1, and FT2 are set equal to zero because there is no contribution from the term $\Gamma_{N\pi}\hat{\Pi}_1$.

Equation 75 is solved in each slice for $S(E, \eta, t)$ by a modified Newton-Raphson method using the values of FT, FT1, and FT2 obtained in the previous slice. An alarm signal is printed out if the subroutine iterates more than 20 times to find a root.

All the integrations involved in the program were performed by using the trapezoidal rule.

The output consists of the matrices PT, PIT, PTINT, and PITINT. The last two represent $\{\hat{N}_1(>E_i, \eta_j, t_k)\}$ and $\{\hat{\Pi}_1(>E_i, \eta_j, t_k)\}$, respectively, and they must be integrated according to Eq. 63 to obtain $\{N_1(>E_i, \eta_j, t_k)\}$ and $\{\Pi_1(>E_i, \eta_j, t_k)\}$. This is achieved by using an auxiliary interpolation-integration program.

Below we give a flow chart (Fig. 23) and a listing of the FORTRAN IV main program and subroutines.

START

READ E0, H2, H3, BETA, N2, N3

INITIALIZE PITINT, X, PT, PIT , N1xN2xN3 MATRICES

ITER=1 , EEO= E0

EPION = 0.185 EEO$^{3/4}$, DELTAE = EEO-EPION,H1=2EPION,N1=$\frac{1}{2}$DELTAE/H1

ITER≥3 ? — YES → N1 = $\frac{DELTAE}{H1}$

NO

ITER>1 ? — YES

NO

FT = FT1 = FT2 = 0

COMPUTE S(E,ETA,T) FOR N1 VALUES OF E ,N2 VALUES OF ETA , N3 VALUES OF T

ITER>1 ? — YES → CALL SUB3 OBTAIN FT, FT1 ,FT2 FOR ALL VALUES OF E,ETA,T

NO

COMPUTE PTINT(I,J,K) N1 x N2 x N3 MATRIX

COMPUTE PT(I,J,K) N1 x N2 x N3 MATRIX

2

RESET INITIAL E, ETA , T

CALL SUB2 , OBTAIN PINT AND THEN PIT(I,J,K) , N1 x N2 x N3 MATRIX

COMPUTE PITINT (I,J,K) , N1 x N2 x N3 MATRIX

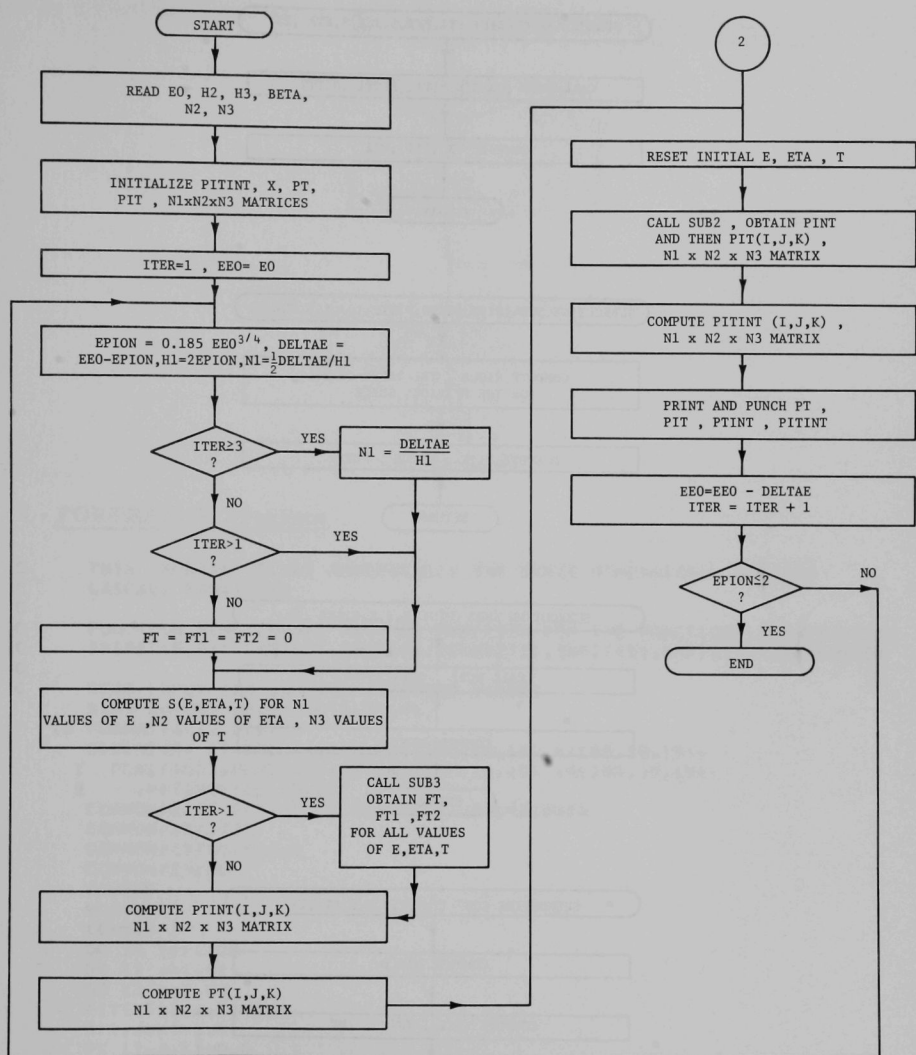PRINT AND PUNCH PT , PIT , PTINT , PITINT

EEO=EEO - DELTAE ITER = ITER + 1

EPION≤2 ? — NO

YES

END

Fig. 23. Flow Chart for FORTRAN IV Program
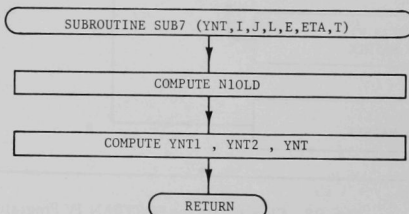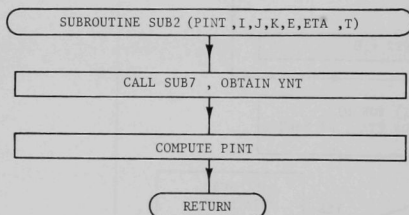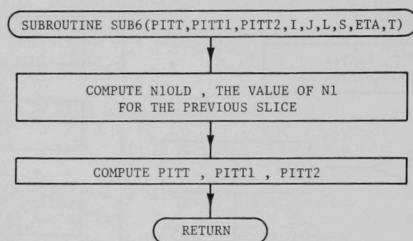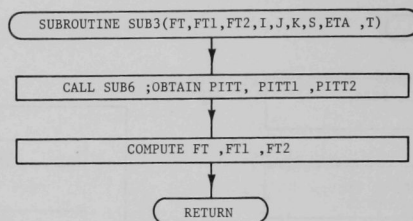
Fig. 23 (Contd.)
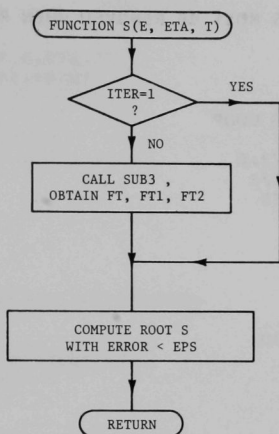
Fig. 23 (Contd.)

3. FORTRAN IV Program

```
C       THIS PROGRAM SOLVES NUMERICALLY THE THREE DIMENSIONAL NUCLEON
C       CASCADE EQUATIONS
C
C       FUNCTION SUBPROGRAMS MUST BE SUPPLIED FOR THE FUNCTIONS SPINT(E,E1),
C       SPIPIT(E,E1),SNNT(S),SNNT1(S),SNNT2(S),SNPIT(S),SNPIT1(S),SNPIT2(5)
C
C       READ IMPUT AND COMPUTE STARTING VALUES
        READ 10,E00,H2,H3,BETA,N2,N3
    10 FORMAT(4E12.0/2I5)
        DIMENSION PT(100,10,15),PIT(100,10,15),P(100,10,15),
     1  FCN1(100),FCN2(100),PTINT(100,10,15) ,X(100,10,15)
     2        ,PITINT(100,10,15)
        COMMON/Z/PT,PIT,N1,N2,N3,EEO,H1,H2,H3,BETA
        COMMON/Z2/ITER
        COMMON/Z3/EO,I,J,K
        COMMON/Z5/UU
        EO=EOC
        ROO=1.1
        TO=0.0
        DO 12 I=1,100
        DO 12 J=1,N2
        DO 12 K=1,N3
        PITINT(1,J,K)=0.0
        X(I,J,K)=1.9
        PT (I,J,K)=0.0
    12 PIT (I,J,K)=0.0
C       EXTERNAL COMPUTING LOOP
        ITER=1
        EEO=EOO
    15 EPION=0.185*EEO**0.75
        DELTAE=EEO-EPION
        H1=2.0*EPION
        N1=0.5*DELTAE/H1
        IF(ITER.GE.3) N1=DELTAE/H1
        IF(ITER.GT.1) GO TO 20
```

66

```
C   THE FOLLOWING 3 CARDS MUST BE REMOVED WHEN PIONS CONTRIBUTION TO NUCLEONS
C   CANNOT BE NEGLECTED
        FT=0.0
        FT1=0.0
        FT2=0.0
C       INTERNAL COMPUTING LOOP
   20 E=EEO-0.5*DELTAE
        IF(ITER.EQ.1) E=E/2.0
        IF(ITER.EQ.1)N1=N1/2
        IF(ITER.GE.3) E=EEO
        DO 100 I=1,N1
        E=E-H1
        UU=X(I,1,1)
        RO=ROO
        DO 100 J=1,N2
        RO=RO-H2
        ETA=-1000.0*ALOG(RO)
        UU=X(I,J,1)
        T=TO
        DO 100 K=1,N3
        T=T+H3
        U=S(E,ETA,T)
        X(I,J,K)=U
        UU=U
        TERM1=(EO/E)**U
        ALEO=ALOG(EO)
        IF(ITER.EQ.1) GO TO 30
C   THE FOLLOWING CARD MUST BE USED ONLY WHEN PIONS CONTRIBUTION TO
C   NUCLEONS CANNOT BE NEGLECTED
        CALL SUB3(FT,FT1,FT2,I,J,K,U,ETA,T)
        TERM=(1.0+FT*EO**(-U))**(-1.0)
        DEN=EO**(-U)*TERM
        DERIV=TERM*ALEO**2+FT2*DEN-(TERM*ALEO+FT1*DEN)**2
        IF(DERIV.LE.0.0) GO TO 30
        GO TO 31
   30 CONTINUE
        DERIV=0.0
   31 CONTINUE
        DENOM=U*(6.2832*(SNNT2(U,ETA,T)+DERIV+1.0/U**2))**0.5
  100 PTINT(I,J,K)=EXP(SNNT(U,ETA,T)-T)*(TERM1+FT*E**(-U))/DENOM
        NN1=N1-1
        DO 98 I=2,NN1
        DO 98 J=1,N2
        DO 98 K=1,N3
        PT(I,J,K)=0.5*(PTINT(I+1,J,K)-PTINT(I-1,J,K))/H1
        IF(PT(I,J,K).LE.0.0) PT(I,J,K)=PT(I-1,J,K)
   98 CONTINUE
        DO 99 J=1,N2
        DO 99 K=1,N3
   99 PT(1,J,K)=PT(2,J,K)
        DO 97 J=1,N2
        DO 97 K=1,N3
   97 PT(N1,J,K)=2.0*PT(NN1,J,K)-PT(N1-2,J,K)
        E=EEO-0.5*DELTAE
        IF(ITER.EQ.1) E=E/2.0
        IF(ITER.GE.3) E=EEO
        DO 101 I=1,N1
        E=E-H1
        RO=ROO
        DO 101 J=1,N2
        RO=RO-H2
        ETA=-1000.0*ALOG(RO)
        T=TO
```

```
      DO 101 K=1,N3
      T=T+H3
      CALL SUB2(PINT,I,J,K,E,ETA,T)
  101 P(I,J,K)=EXP(-0.665*T)*PINT
      DO 134 I=1,N1
      DO 134 J=1,N2
      DO 134 K=1,N3
  134 PIT(I,J,K)=P(I,J,K)
      M=ITER+1
      DO 105 J=1,N2
      DO 105 K=1,N3
      SUM=0.0
      DO 104 I=1,N1
  104 SUM=SUM+PIT(I,J,K)
      PITINT(M,J,K)=PITINT(M-1,J,K)+H1*SUM
  105 CONTINUE
      PRINT 123
  123 FORMAT(20H   SIGNAL   XXXXXXXXXX)
C    PRINT AND PUNCH OUTPUT
      DO 222 K=1,N3
      PRINT 777,N1,H1
      DO 222 I=1,N1
      PRINT 888,(PTINT(I,J,K),J=1,N2)
  222 CONTINUE
      DO 999 K=1,N3
      PRINT 777,N1,H1
      DO 999 I=1,N1
      PRINT 888,( PT(I,J,K),J=1,N2)
  999 CONTINUE
      DO 333 K=1,N3
      PRINT 555,N1,H1
      DO 333 I=1,N1
      PRINT 888,(PIT  (I,J,K),J=1,N2)
  333 CONTINUE
      PRINT 899
      DO 666 K=1,N3
      PRINT 888,(PITINT(M,J,K),J=1,N2)
  666 PUNCH 889,(PITINT(M,J,K),J=1,N2)
  555 FORMAT(20H       PIONS          ,4HN1= ,I3,4HH1= ,E12.4)
  777 FORMAT(20H       NUCLEONS       ,4HN1= ,I3,4HH1= ,E12.4)
  888 FORMAT(10E12.4)
  889 FORMAT(5E12.4/5E12.4)
  899 FORMAT(24H  PION INTEGRAL SPECTRUM)
      EEO=EEO-DELTAE
      ITER=ITER+1
      IF(EPION.LE.2.0) GO TO 21
      GO TO 15
   21 CONTINUE
      RETURN
      END



      SUBROUTINE SUB3(FT,FT1,FT2,I,J,K,S,ETA,T)
      COMMON/Z/PT,PIT,N1,N2,N3,EO,H1,H2,H3,BETA
      COMMON/Z2/ITER
      DIMENSION PT(100,10,15),PIT(100,10,15),FCN(20),FCN1(20),FCN2(20)
      SUM=0.0
      SUM1=0.0
      SUM2=0.0
      DO 200 L=1,K
      X=L
      Y=H3*X-H3
      CALL SUB6(PITT,PITT1,PITT2,I,J,L,S,ETA,Y)
      FACT=EXP(SNNT(S,ETA,Y)-Y)
```

```
      V1=SNPIT (S,ETA,Y)
      V2=SNPIT1(S,ETA,Y)
      V3=SNPIT2(S,ETA,Y)
      U1=SNNT1 (S,ETA,Y)
      U2=SNNT2 (S,ETA,Y)
      FCN(L)=V1*FACT*PITT
      FCN1(L)=FACT*(V2*PITT+V1*PITT1-  V1*PITT*U1)
  200 FCN2(L)=FACT*(V3*PITT+2.0*V2*PITT1+V1*PITT2-U1*(V2*PITT+V1*
     1PITT1)+V1*(     U1**2-  U2))
      IF(K.EQ.1) GO TO 50
      IF(K.EQ.2) GO TO 51
      KK=K-1
      DO 49 L=2,KK
      SUM=SUM+FCN(L)
      SUM1=SUM1+FCN1(L)
   49 SUM2=SUM2+FCN2(L)
      FT=H3/2.0*(FCN(1)+2.0*SUM+FCN(K)) *0.665
      FT1=H3/2.0*(FCN1(1)+2.0*SUM1+FCN1(K))*0.665
      FT2=H3/2.0*(FCN2(1)+2.0*SUM2+FCN2(K))*0.665
      RETURN
   50 FT=0.0
      FT1=0.0
      FT2=0.0
      RETURN
   51 FT=H3/2.0*(FCN(1)+FCN(2)) *0.665
      FT1=H3/2.0*(FCN1(1)+FCN1(2)) *0.665
      FT2=H3/2.0*(FCN2(1)+FCN2(2)) *0.665
      RETURN
      END



      SUBROUTINE SUB6(PITT,PITT1,PITT2,I,J,L,S,ETA,T)
      COMMON/Z/PT,PIT,N1,N2,N3,EO,H1,H2,H3,BETA
      COMMON/Z2/ITER
      DIMENSION PT(100,10,15),PIT(100,10,15),FCN(100),
     1 FCN1(100),FCN2(100)
      SUM=0.0
      SUM1=0.0
      SUM2=0.0
      OLDEO=(EO/0.185)**1.333
      N1OLD=0.25*OLDEO/EO
      IF(ITER.EQ.1) N1OLD=N1OLD/2
      IF(ITER.GE.4) N1OLD=2*N1OLD
      DO 50 M=2,N1OLD
      X=M
      Y=X*H1-H1
      U=ALOG(Y)
      FCN(M)=Y**S*PIT(M,J,L)
      FCN1(M)=FCN(M)*U
   50 FCN2(M)=FCN1(M)*U
      NN=N1OLD-1
      DO 51 M=2,NN
      SUM=SUM+FCN(M)
      SUM1=SUM1+FCN1(M)
   51 SUM2=SUM2+FCN2(M)
      PITT =H1/2.0*(2.0*SUM +FCN (N1OLD))
      PITT1=H1/2.0*(2.0*SUM1+FCN1(N1OLD))
      PITT2=H1/2.0*(2.0*SUM2+FCN2(N1OLD))
      RETURN
      END
```

```
      SUBROUTINE SUB2(PINT,I,J,K,E,ETA,T)
      COMMON/Z/PT,PIT,N1,N2,N3,EO,H1,H2,H3,BETA
      COMMON/Z2/ITER
      COMMON/Z4/TT
      DIMENSION PT(100,10,15),PIT(100,10,15),FCN(20),FCN1(20),FCN2(20)
      TT=T
      SUM=0.0
      DO 50 L=1,K
      X=L
      Y=X*H3-H3
      CALL SUB7(YNT,I,J,L,E,ETA,Y)
   50 FCN(L)=(Y/T)**(BETA/E)*EXP(0.665*Y)*YNT
      IF(K.EQ.1) GO TO 51
      IF(K.EQ.2) GO TO 52
      KK=K-1
      DO 53 L=2,KK
   53 SUM=SUM+FCN(L)
      PINT=H3/2.0*(FCN(1)+2.0*SUM+FCN(K)) *0.665
      RETURN
   51 PINT=0.0
      RETURN
   52 PINT=    H3/2.0*(FCN(1)+FCN(2)) *0.665
      RETURN
      END


      SUBROUTINE SUB7(YNT,I,J,L,E,ETA,T)
      COMMON/Z/PT,PIT,N1,N2,N3,EO,H1,H2,H3,BETA
      COMMON/Z2/ITER
      COMMON/Z4/TT
      DIMENSION PT(100,10,15),PIT(100,10,15),FCN(100)
      IF(ITER.EQ.1) GO TO 52
      OLDEO=(EO/0.185)**1.333
      N1OLD=0.25*OLDEO/EO
      IF(ITER.GE.4) N1OLD=2*N1OLD
      H1OLD=2.0*EO
      SUM1=0.0
      NN=N1OLD-1
      DO 50 N=2,NN
      X=N1OLD-N
      Y1=EO+H1OLD*X
      V1=SPIPIT(E,Y1,ETA,TT,T)
      V2=PIT(N,J,L)
      FCN(N)=V1*V2
   50 SUM1=SUM1+FCN(N)
      YNT1=H1OLD*(SUM1-FCN(2))
      GO TO 53
   52 YNT1=0.0
   53 CONTINUE
      SUM2=0.0
      NN=I
      IF(NN.LE.2) GO TO 51
      DO 49 N=1,NN
      X=N
      Y2=E+H1*X
      U1=SPINT(E,Y2,ETA,TT,T)
      U2=PT(I-N+1,J,L)
      FCN(N)=U1*U2
   49 SUM2=SUM2+FCN(N)
      YNT2=H1/2.0*(2.0*SUM2-FCN(1)-FCN(NN))
      YNT=YNT1+YNT2
      RETURN
   51 YNT=YNT1
      RETURN
```

```fortran
      FUNCTION S(E,ETA,T)
      COMMON/Z/PT,PIT,N1,N2,N3,EEO,H1,H2,H3,BETA
      COMMON/Z2/ITERAT
      COMMON/Z3/EO,I,J,K
      COMMON/Z5/UU
      DIMENSION PT(100,10,15),PIT(100,10,15)
      X=UU
      ALEO=ALOG(EO)
       ARG=ALOG(EO/E)
      EPS=1.0E-4
       ITER=1
   52 CONTINUE
      FACT=2.0*1.385*EXP(-1.385*X)*T+1.0/X-ARG
      DENOM=2.0*(1.385)**2*EXP(-1.385*X)*T+1.0/X**2
      IF(ITERAT.EQ.1) GO TO 53
      EOX=EO**(-X)
      CALL SUB3(FT,FT1,FT2,I,J,K,X,ETA,T)
      DD=1.0+FT*EOX
      TERM1=ALEO-(ALEO+FT1*EOX)/DD
      TERM2=((ALEO**2+FT2*EOX)*DD-(ALEO+FT1*EOX)**2)/DD**2
      FACT=FACT+TERM1
      DENOM=DENOM+TERM2
   53 CONTINUE
      XNEW=X+FACT/DENOM
      DELTA=ABS(XNEW-X)
      IF(DELTA.LT.EPS) GO TO 50
      IF(XNEW.LE.1.E-10) XNEW=ABS(XNEW)+EPS
      IF(XNEW.GT.1.E10) XNEW=EPS
      X=XNEW
      ITER=ITER+1
      IF(ITER.GT.20) GO TO 51
      GO TO 52
   51 PRINT 200
   50 CONTINUE
      S=XNEW
  200 FORMAT(16HALARM DIVERGENCE)
      RETURN
      END



      FUNCTION SNNT (X,RO,T)
      SNNT =          2.0*T*EXP(-1.385*X)
      RETURN
      END



      FUNCTION SNNT1(X,RO,T)
      SNNT1=-1.385* 2.0*T*EXP(-1.385*X)
      RETURN
      END



      FUNCTION SNNT2(X,RO,T)
      SNNT2= 1.92 * 2.0*T*EXP(-1.385*X)
      RETURN
      END



      FUNCTION SNPIT (S,RO,T)
      SNPIT=             T*EXP(-6.21462*S)
      RETURN
      END
```

```
      FUNCTION SNPIT1(S,RO,T)
      SNPIT1=-6.21462*          T*EXP(-6.21462*S)
      RETURN
      END


      FUNCTION SNPIT2(S,RO,T)
      SNPIT2=(6.21462)**2*       T*EXP(-6.21462*S)
      RETURN
      END


      FUNCTION SPINT(E,E1,RO,GAMMA,T)
      A=16.5
      B=2.6
      C=5.55
      SPINT=A/C**2*1.0 /SQRT(E1)*EXP(-B*E/E1**0.75)*(1.0+
     1 (RO*(GAMMA-T)/(C*E))**2)**(-1.5)
      RETURN
      END


      FUNCTION SPIPIT(E,E1,RO,GAMMA,T)
      A=8.3
      B=1.3
      C=5.55
       SPIPIT=         1.0 /SQRT(E1)*EXP(-B*E/E1**0.75)*(1.0+
     1 (RO*(GAMMA-T)/(C*E))**2)**(-1.5)*A/C**2
      RETURN
      END


      DIMENSION PITINT(100,10,15),PI(100,10,15),R(10)
      N1=1
      N2=10
      N3=15
      DO 200 I=1,N1
      DO 200 K=1,N3
      READ 101,(PITINT(I,J,K),J=1,N2)
      PRINT 101,(PITINT(I,J,K),J=1,N2)
  200 CONTINUE
  101 FORMAT(5E12.4/5E12.4)
      R(1)=0.00001
      R(2)=0.0001
      R(3)=0.001
      R(4)=0.002
      R(5)=0.005
      R(6)=0.009
      R(7)=0.01
      R(8)=0.02
      R(9)=0.08
      R(10)=0.1
      DO 201 I=1,N1
      DO 201 J=1,10
      DO 201 K=10,N3
      SUM1=0.0
      RO=1.101
      NN2=N2-1
      DO 202 L=1,NN2
      RO=RO-0.1
```

```
      SUM2=0.0
      DO 203 M=1,100
      X=M
      ROX=X*0.001
      ROXX=RO-ROX
      FACT1=PITINT(I,L+1,K)+(PITINT(I,L,K)-PITINT(I,L+1,K))*10.0*(0.1-
     1 ROX)
      FACT2=-BESJO(-1000.*R(J)*ALOG(ROXX))*ALOG(ROXX)/ROXX
      FACT=FACT1*FACT2
  203 SUM2=SUM2+FACT
  202 SUM1=SUM1+SUM2
      PI(I,J,K)=1.06*SUM1
  201 CONTINUE
C         PRINT OUTPUT
      DO 205 K=10,N3
      PRINT 300
      DO 205 J=1,10
  205 PRINT 301,(PI(I,J,K),I=1,N1)
  300 FORMAT(10H      PIONS)
  301 FORMAT(10E12.4)
      RETURN
      END



      FUNCTION BESJO(X)
      IF(X.GT.3.0) GO TO 51
      U=X/3.0
      BESJO=1.0-2.2499997*U**2+1.2656208*U**4-.3163866*U**6+.0444479*U
     1 **8-.0039444*U**10+.00021*U**12
      GO TO 52
   51 CONTINUE
      V=3.0/X
      F=.79788456-.00000077*V-.0055274*V**2-.00009512*V**3+.00137237*V**
     1  4-.00072805*V**5+.00014476*V**6
      TITA=X-.78539816-.04166397*V-.00003954*V**2+.00262573*V**3
     1  -.00054125*V**4-.00029333*V**5+.00013558*V**6
      BESJO=X**(-0.5)*F*COS(TITA)
   52 CONTINUE
      RETURN
      END
```
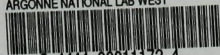
ACKNOWLEDGMENTS

REFERENCES

1. Bruno Rossi, *High Energy Particles*, Prentice Hall, New York (1952).

2. S. V. Starodubtsev and A. M. Romanov, *The Passage of Charged Particles through Matter*, AEC-TR-6468, Washington, D.C. (1965).

3. J. Nishimura, "Theory of Cascade Showers," *Handbuch der Physik, Bd. XLVI/2*, Springer Verlag (1968).

4. *Proceedings, X International Conference on Cosmic Rays. Part I: Invited Papers*, Calgary, Canada (1967).

5. Y. Fujimoto and S. Hayakawa, "Cosmic Rays and High-Energy Physics," *Handbuch der Physik, Bd. XLVI/2*, Springer Verlag (1968).

6. K. R. Symon, *Fluctuations in Energy Loss by High Energy Charged Particles in Passing through Matter*, Ph.D. thesis, Harvard University (1948).

7. U. Fano, Phys. Rev. *92*, 328 (1953).

8. J. Lindhard, M. Scharff, and H. E. Schiott, Mat. Fys. Medd. Dan. Vid. Selsk. *33*, No. 14 (1963).

9. J. B. Sanders, Can. J. Phys. *46*, 455 (1958).

10. J. E. Moyal, J. Math. Phys. *7*, No. 3 (1966).

11. J. E. Moyal, Acta Mathematica *98* (1957).

12. H. E. Schiott, Can. J. Phys. *46*, 449 (1968).

13. J. Lindhard, Mat. Fys. Medd. Dan. Vid. Selsk. *34*, No. 14 (1965).

14. J. E. Moyal, Nucl. Phys. *1*, 180 (1956).

15. J. E. Moyal, Phil. Mag. Ser. 7, *46*, 263 (1955).

16. U. Fano, Phys. Rev. *70*, 44 (1946).

17. U. Fano, Phys. Rev. *72*, 26 (1947).

18. H. Bethe, Ann. d. Physik *5*, 325 (1930).

19. N. Bohr, "The Penetration of Atomic Particles through Matter," *Det. Kgl. Danske Videnskabernes Selskab, Mathematisk-fysiske Meddeleslser XVIII 8*, Copenhagen (1948).

20. W. P. Jesse and J. S. Sadauski, Phys. Rev. *107*, 766 (1957).

21. L. Caneschi and A. Pignotti, Phys. Rev. Letters *22*, 1219 (1969).

22. W. Heisenberg, Z. Physik *113*, 61 (1939) and *126*, 529 (1949).

23. L. Landau, Izv. Akad. Nauk. SSSR *17*, 51 (1953).

24. E. L. Feinberg and A. A. Emel'yenov, articles in Proceedings (Trudy) of the P.N. Lebedev Physics Institute, Vol. 29 (1967).

25. H. Koppe, Z. Naturforsch *3A*, 251 (1948).

26. E. Fermi, Prog. Theor. Phys. *5*, 570 (1950).

27. R. Hagedorn, Suppl. Nuovo Cimento *3*, 147 (1965).

28. R. Hagedorn and J. Ranft, Suppl. Nuovo Cimento *6*, 169 (1968).

29. R. Hagedorn, Suppl. Nuovo Cimento *6*, 311 (1968).

30. G. Cocconi, D. H. Perkins, and L. J. Koester, UCRL-10022 (1961).

31. K. Niu, Nuovo Cimento *10*, 944 (1958).

32. G. Cocconi, Phys. Rev. *111*, 1699 (1958).

33. S. Hasegaua, Progr. Theor. Phys. *26*, 150 (1961) and *29*, 128 (1963).

34. J. R. Wayland and T. Bowen, Nuovo Cimento *48A*, 663 (1967).

35. J. R. Wayland, Phys. Rev. *175*, 2106 (1968).

36. G. Veneziano, Physics Today *22*, No. 9 (Sept 1969).

37. J. L. Day *et al.*, Phys. Rev. Letters *23*, 1055 (1969).

38. G. Zgrablich and J. R. Wayland, Phys. Rev. (1970)(in press).

39. E. I. Daiborg and I. L. Rozental, *XI International Conference on Cosmic Rays*, Budapest (1969).

40. E. Crinó, O. Miguel, A. Fasulo, and G. Zgrablich, *VI Interamerican Seminar on Cosmic Rays*, LaPaz, Bolivia (1970).

41. E. Crinó, O. Miguel, and G. Zgrablich, *VI Interamerican Seminar on Cosmic Rays*, LaPaz, Bolivia (1970).

42. F. Abraham, J. Gierula, R. Levi Setti, K. Rybicki, C. H. Tsao, W. Wolter, R. L. Fricken, and R. W. Huggett, *Multiple Meson Production of Heavy Primary Nuclei of Cosmic Origin and Their Fragmentation Products at Energies above 10^{12} eV*, EFINS 65-44, The University of Chicago, 844 (1965).

43. K. Imaeda, *X International Conference on Cosmic Rays*, HE-34, Calgary (June 1967).

44. R. Hagedorn, TH.1027, CERN, Geneva (Sept 1969).

45. N. Ogita *et al.*, Can. J. Phys. *46*, S164 (1968).

46. K. O. Thielheim and R. Beiersdorf, J. Phys. A (Gen. Phys.) *2*, 341 (1969).

47. D. S. Narayan and G. B. Yodh, Nuovo Cimento *16*, 1020 (1960).

48. L. G. Dedenko, *Proc. Intl. Conf. Cosmic Rays*, EAS 14, London (1965).

49. L. W. Jones *et al.*, invited paper at *X International Conference on Cosmic Ray Physics*, Calgary (1967).

50. N. A. Dobrotin *et al.*, *Proc. Intl. Conf. Cosmic Rays 2*, 817, London (1965).

51. G. Yodh, *A Proposal to Study Strong Interaction Physics Problems from 10^2 to 10^5 GeV on Mt. Chacaltaya in Bolivia*, private communication (1968).

52. C. Cocconi *et al.*, UCRL-10022, p. 167 (1961).

53. A. I. Abrosimov *et al.*, J. Exp. Theor. Phys. *29*, 693 (1955).

54. S. I. Nikolsky *et al.*, Dokl. Akad. Nauk. SSSR *111*, 71 (1956).

55. B. K. Chatterjee *et al.*, Can. J. Phys. *46*, S136 (1968).